Rangarajan, Nagarajan

ESTIMATION OF CARDIOVASCULAR SYSTEM PARAMETERS USING NONINVASIVE MEASUREMENTS

Iowa State University PH.D. 1983

PLEASE NOTE:

In all cases this material has been filmed in the best possible way from the available copy. Problems encountered with this document have been identified here with a check mark ✓.

1. Glossy photographs or pages ✓
2. Colored illustrations, paper or print _____
3. Photographs with dark background ✓
4. Illustrations are poor copy _____
5. Pages with black marks, not original copy _____
6. Print shows through as there is text on both sides of page _____
7. Indistinct, broken or small print on several pages _____
8. Print exceeds margin requirements _____
9. Tightly bound copy with print lost in spine _____
10. Computer printout pages with indistinct print _____
11. Page(s) _____ lacking when material received, and not available from school or author.
12. Page(s) _____ seem to be missing in numbering only as text follows.
13. Two pages numbered _____. Text follows.
14. Curling and wrinkled pages _____
15. Other _____

Estimation of cardiovascular system parameters using noninvasive measurements

by

Nagarajan Rangarajan

A Dissertation Submitted to the
Graduate Faculty in Partial Fulfillment of the
Requirements for the Degree of
DOCTOR OF PHILOSOPHY

Departments: Engineering Science and Mechanics
Biomedical Engineering
Co-majors: Engineering Mechanics
Biomedical Engineering

Approved:

Signature was redacted for privacy.

In Charge of Major Work

Signature was redacted for privacy.

Professor-in-charge,
Program in Biomedical Engineering

Signature was redacted for privacy.

For the Major Department

Signature was redacted for privacy.

For the Graduate College

Iowa State University
Ames, Iowa

1983

TABLE OF CONTENTS

CHAPTER 1. INTRODUCTION

Arteries serve as conduits that carry blood, rich in oxygen and other nutrients, to the various parts of the body. An unobstructed artery is capable of meeting the blood flow requirements of the body at rest, or during exercise, when the flow requirements are increased. Atherosclerosis is a disease that leads to progressive narrowing of the arteries due to a build up of plaque along the vessel wall. An arterial obstruction is commonly called a stenosis. The narrowing of an artery can lead to problems when the artery cannot meet the resting, or elevated, flow requirements of the parts of the body perfused by it. Frequently, the obstruction of an artery can lead to death, and arterial diseases are the leading cause of functional impairment and death in the United States. This fact has created much interest in quantitative analysis of the functioning of the cardiovascular system in normal and diseased states. Thus, a significant part of current cardiovascular research is directed towards achieving both a qualitative and quantitative understanding of the dynamics of the cardiovascular system.

The complexity of the cardiovascular system and the difficulties encountered in identifying and measuring, in vivo, the various system variables have led to an effort to construct models of the system. These models incorporate the basic features of the system and are usually developed by making a variety of simplifying assumptions about the behavior of the system. Also, the models, which may be physical, mathematical or computer based, enable the researcher to better understand the dynamics

of the complicated system, and to identify important parameters in the system.

The behavior of a physical system can often be described by a set of differential equations. These equations are then said to constitute a mathematical model of the physical system. Typically, the one-dimensional flow equations, together with an equation of state for the vessel, have been used to describe, mathematically, the flow of blood in the larger arteries. The equation of state is used to relate the cross-sectional area of the artery and the pressure. This set of partial differential equations, which necessarily incorporates a number of simplifying assumptions, constitutes a mathematical model which can be used to study the dynamics of blood flow in a section of a normal or stenosed artery.

This model describing arterial blood flow is usually written in terms of variables such as the pressure and the flow in the artery. It contains important cardiovascular system parameters such as the compliance of the artery (the increase in cross-sectional area per unit increase in pressure), arterial diameter and length, the location and the inner diameter of any stenoses that may be present, and parameters pertaining to blood (viscosity and density). Of these various parameters, it is generally possible to measure the density and the viscosity of blood directly. However, the compliance and the radius of the artery, and parameters pertaining to the stenosis such as its location and severity cannot be easily determined by direct in vivo measurements. Recently, some research effort has been directed towards obtaining, indirectly, reasonable estimates for these parameters by using dynamic measurements of the system

variables. Such procedures are commonly referred to as parameter estimation techniques.

In using parameter estimation, the system parameters are initially set at some assumed values and certain measured values of the system variables are used as input for the model. The output from the model is then compared with corresponding data measured experimentally. An algorithm is constructed to vary the system parameters in a systematic manner to minimize the sum of the square of the difference, S, between the measured data and the output from the model. The values of the parameters which minimize S are taken to be the best estimates for the parameters in the model. Thus, parameter estimation is a technique which can be used to estimate certain model parameters by using the values of system variables which are amenable to direct measurement, and thus can be a very useful tool in biology and medicine.

In the case of the cardiovascular system, variables which can be measured directly are flow and pressure in the various sections of the artery. However, a common problem is one of obtaining accurate measurements of these variables. Pressure transducers and electromagnetic flowmeters are commonly used to obtain these measurements, but the use of these transducers involves surgery and these measurements are termed "invasive." In a clinical situation, the physical condition of the patient may preclude the possibility of obtaining invasive measurements, and invasive data acquisition may be time consuming. Also, the trauma associated with invasive measurements can interfere with the normal behavior of the biological system. The disadvantages of invasive measure-

ments, as detailed above, reveal the importance of developing new techniques for the measurement of flow and pressure. In the past, a few studies based on parameter estimation techniques and utilizing invasive measurements have been used to determine arterial system parameters.

The relatively recent introduction of the ultrasonic Doppler flowmeter has made it possible to measure, noninvasively and with reasonable accuracy, the instantaneous cross-sectional averaged velocity of blood in an artery. Also, recent technological advances suggest that it may be possible to obtain pressure waveforms from noninvasively measured changes in the diameter of an artery as blood pulses through it, where the changes in the diameter can be measured ultrasonically. The improvements in noninvasive measurement techniques and the usefulness of parameter estimation techniques raises the question as to whether noninvasive measurements of the system variables can be used to estimate important system parameters. The aim of this study is to answer this question by systematically exploring the possibility of obtaining reasonably accurate noninvasive measurements of pertinent system variables, and using these measurements in an estimation scheme.

The study was carried out in two phases. In phase one, tests were conducted on a hydraulic model simulating a segment of the artery containing a stenosis. The aim of this phase was to develop and validate the necessary instrumentation and experimental techniques, and to establish a suitable parameter estimation technique. In phase two, limited experiments were carried out on the femoral arteries of mongrel dogs to

determine if the mathematical model and the procedures used in phase one could be used to predict stenosis parameters in the dog.

In phase one, the arterial segment was simulated by using latex tubing of various wall thicknesses. The tube was fixed in the axial direction and remained free to expand and contract in the radial direction. A syringe pump was used to create pulsatile flow in the tube. The upstream (proximal) and downstream (distal) flow in the tube was measured invasively by using electromagnetic flowprobes. The corresponding pressures were measured using pressure transducers. Concurrently, the flow and the pressures were also measured noninvasively using ultrasonic instrumentation.

In order to fulfill the aims stated above, phase one was further divided into the following parts:

1. In part one, an ultrasonic transducer was used to determine the compliance of an unobstructed tube and this value was compared with directly measured value.
2. In part two, the invasively measured data from an unobstructed tube were used in the parameter estimation scheme to predict system parameters such as the compliance of the tube and distal resistance to flow. Estimated values of the parameters using noninvasive data were compared with corresponding values obtained using invasive data.
3. In part three, a rigid annular plug of known inner diameter was used to model a discrete stenosis and both invasive and noninvasive measurements obtained. Estimated stenosis parameters based on noninva-

sive measurements were compared with those obtained using invasive measurements.

As noted previously, in phase two, experiments were carried out using large mongrel dogs. The femoral artery of each dog was exposed and a rigid annular plug of known inner diameter was introduced into the artery to simulate an axisymmetric stenosis in the artery. Invasive pressure and flow measurements were obtained from the test section of the femoral artery and used to estimate the location and the severity of the stenosis. The estimated values of these parameters were compared to the corresponding experimentally measured values.

CHAPTER 2. LITERATURE REVIEW

The complexity of the cardiovascular system and the difficulties encountered in obtaining accurate measurements of the various system parameters has led to much research into the use of models to represent the system. Some examples of such modeling efforts include the Windkessel model, transmission line models, and models based on the Navier-Stokes equations. The common aim of these past modeling studies has been to predict as closely as possible the physiological behavior of the system. Once a model has been developed, its validity is normally tested by comparing pressure and flow wave shapes generated by the model with the corresponding data obtained from human or animal experiments. This approach to validation is feasible only when all the model parameters can be measured directly or can be approximated reasonably well.

The mathematical model contains parameters such as the compliance of the tube, tube diameter and parameters pertaining to stenoses such as its location and severity. It is difficult to measure these parameters directly in a physiological system. Under these circumstances, parameter estimation techniques have been used to estimate the unknown parameters by using measured values of the system variables such as pressure and flow in the arterial segment as input to the model. Some research has been undertaken to measure the system pressure and flow noninvasively by using ultrasonic measurement technology.

In this chapter, some of the past research efforts in the areas of mathematical modeling, the application of the parameter estimation schemes

to cardiovascular systems, and the noninvasive measurement of flow and pressure waveforms in the arterial system will be reviewed.

Mathematical Modeling

The basic feature that needs to be modeled is an unobstructed segment of the artery which is free of branches. It has been observed that whole blood tends to behave like a Newtonian fluid for high shear rates, and has a viscosity in the range of 0.003 to 0.004 N-s/m^2 (Caro et al., 1978). Blood can also be assumed to be incompressible for the range of pressures encountered in the arterial system. Under these conditions, the Navier-Stokes equations can be used to describe the pulsatile motion of the blood in the arteries. These equations in their full form are very complex. A consideration of the architecture of the arterial system suggests that the following assumptions can be made in order to arrive at a relatively simple working model:

1. An artery can be described as a straight, distensible, and slightly tapered tube with a circular cross-section.
2. The vessel is totally constrained in the axial direction.
3. The vessel wall is incompressible and behaves in a linearly elastic manner.

Using the above mentioned assumptions, it is possible to model blood flow in a segment of the artery by using the one-dimensional flow equations. This approach has been successfully used by several authors in the past (Streeter et al., 1963; Olsen and Shapiro, 1967; Anliker et al., 1971a,b; Schaaf and Abbrecht, 1972; Wemple and Mockros, 1972; Raines

et al., 1974; Rumberger and Nerem, 1977; Rooz, 1980; Young et al., 1980; Gray, 1981). The equations of continuity and axial momentum can be written as

$$\frac{\partial Q}{\partial x} + \frac{\partial A}{\partial t} = 0 \tag{2.1}$$

$$\frac{\partial Q}{\partial t} + \frac{\partial}{\partial x}(\lambda Q^2/A) = -\frac{A}{\rho}\frac{\partial p}{\partial x} + \frac{\tau_0 \pi D}{\rho} \tag{2.2}$$

where

$Q(t,x)$ = flow at time t at an axial location x

$p(t,x)$ = pressure at time t at an axial location x

A = lumen area

D = lumen diameter

τ_0 = wall shearing stress

ρ = blood density

λ = one-dimensional momentum flux coefficient

The coefficient, λ, can be represented by

$$\lambda = \frac{1}{A}\int_A \left(\frac{v_z}{V}\right)^2 dA \tag{2.3}$$

where v_z and V are the axial component of the velocity, and the instantaneous mean flow velocity, respectively. To complete the formulation of the model, it is necessary to prescribe a relationship between the pressure and the area. This is usually referred to as the "equation of state" of the vessel and takes the form

$$A = A(p(x,t),x) \tag{2.4}$$

It is pertinent to note that this form for the equation of state allows for geometric tapering of the vessel and for the vessel to be distended in an arbitrary fashion by the transmural pressure. However,

it excludes viscoelastic behavior of the wall. This is a simplification of the real mechanical properties of the vessel wall. Some researchers (Westerhof and Noordergraaf, 1970; Noordergraaf, 1978) have proposed simple viscoelastic models to simulate the properties of the wall. Holenstein and Niederer (1980) have proposed a model using a complex-valued creep function. These models generally suffer from a lack of adequate reliable data.

The simplest form of the equation of state assumes that the cross-sectional area is a linear function of the pressure and that the changes in the area are relatively small as compared to some reference area. This can be expressed mathematically as

$$A(p,x) = A_0 + C(x)(p - p_0) \tag{2.5}$$

with

$$|C(x)(p - p_0)| \ll A_0(x) \tag{2.6}$$

where $A_0(x)$ is the cross-sectional area at some reference pressure p_0 and $C(x)$ is the vessel compliance per unit length. This form of the equation of state has been used by many researchers (Noordergraaf et al., 1964; Taylor, 1965; Snyder and Rideout, 1968; Westerhof et al., 1969; Welkowitz, 1977; Young et al., 1980; Gray, 1981).

Raines et al. (1974) used an equation of state of the form

$$A(p,x) = A_0(x) + b \ln(p/p_0) \tag{2.7}$$

In this equation, $A_0(x)$ was determined by fitting a curve to angiographic data, and b was assumed to be a constant over a limited length of artery (and obtained experimentally).

Streeter et al. (1963) derived the equation of state from an analysis of stresses within thin-walled vessels. The equation of state derived by him and also used by other researchers (Schaaf and Abbrecht, 1972; Wemple and Mockros, 1972) takes the form

$$A/A_0 = 1/(1 - (pD/hE)) \tag{2.8}$$

In this equation, E is Young's modulus for the wall material and h is the wall thickness.

Anliker et al. (1978) and Stettler et al. (1981) proposed the following form for the equation of state:

$$A(p,x) = A_0(x)\exp \frac{p - p_0}{\rho c(p,x)c(p_0,x)} \tag{2.9}$$

where c, the wave speed of small distension, was obtained experimentally.

Rooz (1980) conducted experiments on latex tubing and fitted the data in the form

$$A = A_0 + B(p - p_0) + C(p - p_0)^2 \tag{2.10}$$

where B and C are constants.

The nonlinear term in Eq. (2.2) is the one pertaining to convective acceleration. Schaaf and Abbrecht (1972) computed the magnitudes of the individual terms of the momentum equation over one pulse cycle for the proximal radial artery and the proximal thoracic aorta. They found that the momentum flux term was small compared to the other terms at both the sites.

The wall shear stress term, τ_0, in the momentum equation has been modeled in many ways. The simplest approach is to approximate the wall shear stress using a Poiseuille flow friction term, i.e.,

$$\tau_0 = - \frac{8\mu Q}{AD} \tag{2.11}$$

This approach has been used by Raines et al. (1974), Rooz (1980), Gray (1981), Stettler et al. (1981) and Young et al. (1980).

Schaaf and Abbrecht (1972) used an approximation derived from steady-oscillatory flow solution for an infinite, rigid and uniform tube. The wall shear term then takes the form

$$\tau_0 = - \frac{8\mu V}{D} + \frac{\rho D(\lambda - 1)}{4} \frac{\partial V}{\partial t} \tag{2.12}$$

where V is the instantaneous mean flow velocity, λ is the one-dimensional momentum flux coefficient and takes the values 1 for flat velocity profile and 4/3 for parabolic velocity profile. These authors found that setting $\lambda = 1$ produced only small changes in the results. Also, when the value of λ was set to 1 and the viscosity, μ, was set to 0, the overall behavior of the model did not change appreciably. It can, thus, be concluded that the friction terms are of secondary importance in determining the behavior of large arteries and Eq. (2.11) is a reasonable approximation for the friction term.

Thus, a linear system of equations can be obtained by assuming that:

1. The cross-sectional area is a linear function of the pressure, and changes in area are relatively small.
2. The friction term can be modeled by Eq. (2.11).
3. The convective acceleration term can be neglected.

The continuity and the momentum equations can, thus, be written in a linearized form as

$$\frac{\partial Q}{\partial x} + C \frac{\partial p}{\partial t} = 0 \tag{2.13}$$

$$\frac{\partial p}{\partial x} + RQ + L \frac{\partial Q}{\partial t} = 0 \tag{2.14}$$

where $R = 8\pi\mu/A_0^2$ and $L = \rho/A_0$.

As noted previously, a constriction in the artery is termed a stenosis. The factors which cause a stenosis to develop in an artery are not well-understood and are the subject of much research. Stenoses are usually created by the build-up of atherosclerotic plaques which protrude into the lumen of the artery. The presence of a stenosis in an artery can reduce blood flow to the distal beds being perfused by that artery. This in turn can cause functional impairment or death.

To understand the effect of a stenosis on the flow of blood, several attempts have been made to model the stenosis. Young and Tsai (1973a,b) studied the pressure drop across isolated axisymmetric and nonsymmetric constrictions. They approximated the pressure drop across a constriction in an unsteady flow by the relationship

$$\Delta p = K_u \frac{\mu}{D} U + \frac{K_t}{2} \left(\frac{A_0}{A_1} - 1\right)^2 \rho |U| U + K_u \rho L_s \frac{dU}{dt} \qquad (2.15)$$

where

K_u = an empirical constant

K_v = an empirical constant

K_t = an empirical constant

A_0 = the unobstructed cross-sectional lumen area

A_1 = the minimum cross-sectional area of the constriction

U = the instantaneous velocity in the unobstructed tube averaged over the cross-section

ρ = the fluid density

D = the diameter of unobstructed tube

L_s = the length of the stenosis

The first term on the right hand side of the equation accounts for the viscous effects, the second term accounts for convergence and divergence effects, and the third term accounts for unsteady effects. Both K_u and K_t appear to be only slightly dependent on the geometry. Both of these coefficients could be approximated from steady flow tests. K_v was obtained empirically. In subsequent experiments, Young et al. (1975) introduced artificial stenoses in the femoral artery of dogs. The stenoses were in the form of cylindrical hollow plugs made of rigid material. They found that Eq. (2.15) could be used to satisfactorily estimate the pressure drops across an arterial stenosis. Seeley and Young (1976) proposed that the value of K_v could be approximated by

$$K_v = 32\left(\frac{L_a}{D_0}\right)\left(\frac{A_0}{A_1}\right)^2 \tag{2.16}$$

with

$$L_a = 0.83L_s + 1.64D_1 \tag{2.17}$$

where

L_a = the corrected length of the stenosis

D_1 = the inner diameter of the stenosis

A_1 = the cross-sectional area of the stenosis

D_0 = the lumen diameter

A_0 = the lumen cross-sectional area of the unobstructed tube

They also found that K_t could be approximated well by a value of 1.52 for blunt axisymmetric constrictions. Young (1979) observed that the pressure drop across blunt axisymmetric constrictions in an artery could adequately

be approximated by using Eq. (2.12) with the values of K_t and K_u being set at 1.52 and 1.2, respectively, and with the value of K_v given by Eq. (2.16).

Anliker et al. (1978) proposed a similar equation for the pressure drop across an axisymmetric constriction. The equation proposed by them was the form

$$\Delta p = \frac{\rho}{2}(v_2^2 - v_1^2) + \rho \int_{r_1}^{r_2} (\frac{\partial v}{\partial t})dx + \frac{\rho}{2} v_1^2(\frac{A_0}{A_1} - 1)^2 + \frac{8\pi\mu L_s}{A_1}(\frac{A_0}{A_1})v_1 \qquad (2.18)$$

Other efforts at modeling stenosis have been carried out by Newman et al. (1979).

Equations (2.13) and (2.14) constitute a set of differential equations which are used to model the flow of blood in an unobstructed artery. Many different approaches have been used to solve this set of equations. Snyder and Rideout (1968) and Westerhof et al. (1969) set up an electrical analog of this model and solved it by direct analog computation. The method of characteristics has been used by many researchers (Streeter et al., 1963; Olsen and Shapiro, 1967; Wemple and Mockros, 1972; Vander Werff, 1974; Anliker et al., 1978). Raines et al. (1974) used the finite difference technique to solve this model and Olsen and Shapiro (1967) used the method of perturbations. The finite element method has been used by Rooz (1980) and Gray (1981) to solve Eqs. (2.13), (2.14) and (2.15) for flow of blood through a stenosed artery, and this is the method used in the present study. Further details are presented in a later section.

Noninvasive Measurements of Pressure

In man, traditional methods such as the ausculatory method have been used to measure peripheral systolic and diastolic blood pressures. Such methods are limited in their application to certain parts of the anatomy where the arterial sounds can be heard distinctly, and cannot be used to measure the pressure over an entire cycle of the pressure pulse. Measurement of diastolic pressures by conventional means also suffers from inaccuracies. As noted at the beginning of this chapter, measured pressure pulse data are required as input and output data in the estimation scheme.

Few studies on the noninvasive measurement of pressure have been reported. Raines et al. (1973) developed a recorder which yielded an accurate recording of the entire pressure pulse. Hokanson et al. (1972) used a phase-locked echo tracking system to record, noninvasively, the changes in the arterial diameter as the blood pulses through it. The phase-locked echo tracker (UET) developed by them is capable of measuring changes in the diameter of the artery in the range of 0.002 mm, whereas the diameter of the artery can be read to an accuracy of 0.1 mm. Mozersky et al. (1972) used the UET to measure the elastic properties of the human femoral artery. The pressure-strain elastic modulus of the human femoral artery and the external iliac arteries obtained by using the UET was found to be quite similar to the values previously reported by other authors using other techniques.

It is pertinent to note that the contour of the arterial wall-displacement pulse recorded with the UET is nearly identical to that of the pressure pulse. It will be seen later that it is possible to transform

the arterial wall-displacement pulse waveform into the pressure pulse waveform by using a suitable transformation relationship.

Noninvasive Measurement of Velocity

Doppler velocimeters were developed by Satomura (1959). These instruments transmit a beam of ultrasound of constant frequency from a transmitter. The ultrasound scattered by the insonated structures is received by a receiver adjacent to the transmitter. If the insonated structures are moving, the frequency of the received ultrasound will be changed by an amount proportional to their velocity. Thus, the difference between the frequency of the emitted and received ultrasound is an indication of the velocity of the moving structures. If the transmitted beam insonates an artery, the red blood cells which are moving scatter the ultrasound and cause a frequency shift. If a single moving cell is insonated, its velocity can be calculated by the Doppler equation

$$V = fc/2F\cos\alpha \tag{2.19}$$

where

f = difference in frequency between the transmitted and the received ultrasound

F = frequency of the transmitted ultrasound

c = the velocity of sound in blood

α = the angle between the ultrasound beam and the axis of the artery

Lunt (1975) carried out an extensive analysis of the accuracy and the limitations of the Doppler flowmeters incorporating zero crossing detectors. He suggested that in spite of all its limitations, these

instruments are capable of measuring the velocity of blood to about 20% accuracy and can detect changes in velocity of about 5%.

Bernstein et al. (1970) suggested that directionally sensitive Doppler flowmeters are very good noninvasive diagnostic tools. They indicated that the flowmeter could be used to diagnose occlusive arterial diseases and chronic veinous diseases. Doppler flowmeters could also be used to monitor patients during and after vascular reconstruction operations.

Reagen et al. (1971) measured the blood flow in the femoral artery transcutaneously. In order to do this, they used a UET to obtain the diameter of the vessel and a directional Doppler flowmeter (USF) to obtain the cross-sectional averaged flow velocities. They found that the calculated volume flow rate from their experiments agreed with those measured by using indicator dilution methods.

Shoor et al. (1979) confirmed the findings of Lunt (1975). They found that the blood velocities measured by the USF were within 5% of that measured by electromagnetic flowmeters (EMF) in in vitro conditions. They also suggest that the USF could be routinely used to provide quantitative measurements of blood flow with an accuracy of 10% to 20%. Similar results have been reported by Moss and Bennett (1979).

Hankner (1978) compared the flow waveform obtained from the USF and the EMF and found that the waveforms obtained by both these methods were comparable for low velocities and pulse frequencies. He suggested that the limitations in the performance of the USF would prevent an accurate

measurement of the flow waveform in physiological conditions when the peak cross-sectionally averaged velocities exceeded approximately 0.8 m/s.

These past studies thus suggest that with careful measurement techniques, it may be possible to use the USF and the UET to measure noninvasively (and with reasonable accuracy) the instantaneous cross-sectionally averaged velocity of blood and the changes in the diameter of the artery. A transformation can be used to transform the vessel wall-displacement pulse into the arterial pressure pulse. Ultrasonic measurement techniques thus make it possible to measure noninvasively pressure and flow waveforms which can be used as input quantities in a parameter estimation scheme.

Parameter Estimation Technique

Once a realistic mathematical model of the arterial segment has been prescribed, it can be used in two different ways. It can be used as a research or predictive tool in which the model parameters can be changed and their effects on flow variables observed and tabulated. This could lead to a better understanding of the functioning of the system in abnormal or diseased states. The model can, however, also be used as a diagnostic tool.

The process of diagnosis in a physiological situation involves the analysis of symptoms in order to decide on the nature of the disease conditions. The symptoms that usually characterize the build up stenosis in an arterial system are significant changes in arterial flow and pressure. Thus, by analyzing the flow and the pressures in an arterial segment, it

should be possible to draw some conclusions about the presence or absence of a stenosis. However, the most common diagnostic tool for obtaining specific information about the stenosis, such as its severity and its location, is arteriography, an invasive technique.

Parameter estimation is another potential method for obtaining the information pertaining to the stenosis. In this method, system variables which are amenable to measurement, such as the flow and the pressure, are used as input data for the model. As described previously, the unknown parameters in the model are set at a given value and the model is solved. The values of the system variables predicted by the model are then compared with the directly measured values of the corresponding variable, and the difference between the measured value of a variable and its value as predicted by the model is minimized by systematically varying the values of the unknown system parameters. The model is said to be optimally adjusted when this error is minimum. The values of the system parameters which yield such an optimal adjustment are called the "best estimates." Thus, it is possible to estimate indirectly parameters which cannot be measured directly by using directly measured values of other system variables.

Theoretically, parameter estimation is an excellent diagnostic tool, and it is reasonable to expect that it would be widely used in the biological field where one encounters a large number of parameters which are difficult to measure. However, such has not been the case. Rideout and Beneken (1975) and Bekey and Yamashiro (1976) present a survey of the applications of the parameter estimation methods in the physiological

disciplines. These authors have indicated the reasons why the parameter estimation schemes have not found a wider acceptance in the biological field. Some of the reasons cited by the authors which are particularly relevant to this study are:

1. The difficulty in designing good experiments in order to obtain good input-output data for the parameter estimation schemes.
2. The problem of obtaining accurate measurements of the system variables.
3. Problems associated with prescribing reasonably accurate mathematical models to represent a biological system realistically.
4. The nonlinearities in the system which lead to nonunique estimates of the parameter values.
5. The high cost of computation associated with most parameter estimation schemes.

Although there are obvious difficulties, several previous studies involving parameter estimation have been reported.

Sims (1972) used a 10 compartment analog model of the arterial system of a dog. He used Marquardt's scheme to estimate 13 parameters (compliances and peripheral resistances) in the model. The estimates were based on 2 invasive flow and 3 pressure measurements made at various sites along the arterial tree. Model-to-model tests to validate the estimation scheme converged in 8 iterations. The estimates for most of the parameters of interest were satisfactory. However, there were large errors in the estimated values of two peripheral resistances and a compliance. He

also mentions that a very large amount of computer time was required to obtain convergence in the model-to-model tests.

Wesseling et al. (1973) used a least-squares error criterion to estimate the radius and compliance of an artery, the inertance of the various segments along the artery, and the peripheral resistance in a lumped linear four segment model. The input and output data for the estimation scheme consisted of uncalibrated recordings of the pressure pulse taken at the brachial artery and the radial artery, respectively. They attempted to match the output from the model with the pulse waveform at the radial artery by varying the system parameters manually. Each model parameter was adjusted independently in order to obtain a match. They found that the estimates for the parameters fell within the physiological range.

Chang et al. (1974) used a lumped analog model. They used the Hooke-Jeeves pattern search method to optimize the parameters. An invasively obtained pressure waveform was used as the input to the parameter estimation scheme. Two pressure and two flow waveforms were used for comparison and matching. They attempted to estimate the radii and the length of the vessels, the elastic modulus of the vessels and the resistances in each section. Model-to-model tests yielded good results. However, a large number of iterations were required to obtain the optimum values of the parameters.

Bourne and Kitney (1978) developed a 11 compartment model of an artery. Included in the model were 3 branches. They used a modified form of the Rosenbrook method, a direct search method, to optimize the values

of the parameters. Measured aortic flow was the input into the estimation scheme and measured arterial pressure was used for comparison and model fitting. They attempted to estimate the overall arterial compliance and the total peripheral resistance. Model-to-model tests yielded reasonably good results. The authors also tried to quantify the effects of noise in the measured values of the input and output data. Such an analysis is particularly relevant in a clinical situation where there is invariably some noise superimposed on measurements, and the use of such noisy data as input or output to the estimation scheme will lead to inaccurate estimates for the system parameters. The authors superimposed randomly generated white noise on the pressure waveform used for model fitting. They found that the errors in the estimated values of the parameters when noisy data were used for model fitting was comparable to noise added to the pressure wave form. It was also seen that the estimated values of the compliance were quite sensitive to the noise in the pressure data. The estimates for the peripheral resistance, however, did not vary significantly when noise was added to the pressure data.

Clark et al. (1980) used a modified 2 compartment Windkessel model of the arteries. They estimated the lumped viscoelastic properties of the aorta and the large arteries, the compliance of the systemic circulation, the inertance of the fluid columns connecting the two compartments and the initial flow. The pressures in the left ventricle, the ascending aorta and the brachial artery were used as inputs into the estimation scheme. Proximal and distal pressures in the system were used for comparison and model fitting. A set of initial guesses for the parameter values was

chosen by using a modified Prony method and the Marquardt scheme was used for the estimation of the parameters. The model-to-model tests yielded good results and the model-to-human tests yielded physically reasonable estimates.

Young et al. (1980) used the finite element method to solve the mathematical model of pulsatile flow in flexible tubes. They used a least squares estimation procedure incorporating the Gauss-Newton linearization scheme to predict the various model parameters. The flow system was modeled physically using a simple hydraulic model from which flow and pressure data for input to the estimation scheme were obtained. The authors investigated the effects of using different sets of boundary conditions to solve the model and the use of different input data, such as, the proximal and distal pressures and flows for optimization of parameters. They found that the flow-flow or the flow-resistance boundary conditions when used with the proximal or distal pressure waveform for comparison and model fitting yielded the most reliable estimates for the system parameters. Their study indicated that the solution of the model is not very sensitive to changes in some system parameters such as the radius of the tube. These parameters could not, therefore, be estimated accurately. The compliance of the tube and the peripheral resistance were estimated within 10% of the measured experimental values.

Gray (1981) used a mathematical model to describe pulsatile flow through a flexible tube with a branch. Initially, he attempted to estimate the severity and the location of the stenosis in a straight tube without branches. The proximal flow and distal pressure data obtained

from a hydraulic model were used as boundary conditions to solve the model. The distal flow and the proximal pressure were used for comparison and model fitting in the parameter estimation scheme. He used an ordinary least squares scheme incorporating the Gauss-Newton linearization method to optimize the parameter values. Model-to-model tests to validate the estimation scheme yielded very accurate estimates for the parameters. In the model-to-experiment tests, when a stenosis representing an area reduction of 90% was introduced in the flow field, the estimates for the area reduction and the location of the stenosis were within 10% and 17%, respectively, of the experimentally measured values. With a stenosis representing an area reduction of 75% located midway between the proximal and distal measurement sites, he was able to obtain an estimate for the area reduction which was within 13% of the experimentally measured value. He was unable to obtain a reasonable estimate for the location of the stenosis in this case. He then conducted similar tests on a branched tube. The proximal flow and the peripheral resistance of the branch and the main tube were used as boundary conditions to solve the model. The proximal pressure and the distal flow in the main tube were used for comparison and model fitting. When a stenosis representing 90% area reduction was introduced in the flow field in the main tube, reasonably accurate estimates were obtained for the values of the compliance of the main tube and the severity and the location of the stenosis. Based on the results of the model-to-model tests, he attributed the discrepancy between the estimated and measured values of the parameters in model-to-experiment tests to inaccuracies in measurements and modeling errors.

A perusal of the above literature review indicates that considerable research has been done in the areas of mathematical modeling of pulsatile flow in segments of arteries, and noninvasive measurements of flow and pressure waveforms. Some work has been done in the application of the parameter estimation techniques to predict important parameters in the cardiovascular system. Gray (1981) has been able to establish some bounds on the errors to be expected when the ordinary least squares estimation technique is used to estimate the parameters in a hydraulic model of the flow in a segment of the artery.

The purpose of the present work is to attempt to extend and integrate various aspects of these past studies, and to systematically investigate the possibility of estimating some of the critical parameters in the mathematical model based on noninvasively obtained measurements.

CHAPTER 3. THEORETICAL ANALYSIS

The survey of pertinent literature in the previous section indicates that the flow of a fluid in an obstructed tube can be represented mathematically by the continuity equation, the linearized axial momentum equation, a linear equation of state, and an empirically derived equation giving the pressure drop across the constriction. This set of equations was solved using the finite element method.

The discretization of the solution domain, the formulation of element coefficient matrix and the assembly of the global stiffness matrix follow essentially along the lines suggested by Rooz (1980). Some changes were made in the formulation of the global matrix to account for the fact that the length of the stenosis may be different from the length of the elements in the unobstructed sections of the tube. Some minor changes were also made in the values of some of the elements of the element coefficient matrix.

A summary of the mathematical model used, the numerical solution procedure and the parameter estimation scheme will be given in this chapter.

Mathematical Model

The flow geometry investigated in this study is given in Fig. 3.1. The following assumptions are made in order to arrive at a set of linearized partial differential equations describing the pulsatile flow of a Newtonian fluid in a flexible tube:

Fig. 3.1A. Layout of straight unobstructed tube

Fig. 3.1B. Layout of stenosed tube

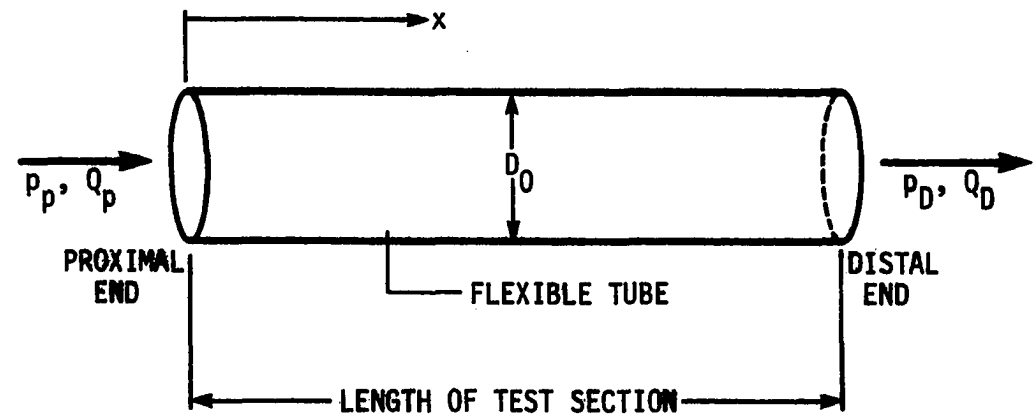
x
D_0
p_p, Q_p
p_D, Q_D
PROXIMAL END
FLEXIBLE TUBE
DISTAL END
LENGTH OF TEST SECTION

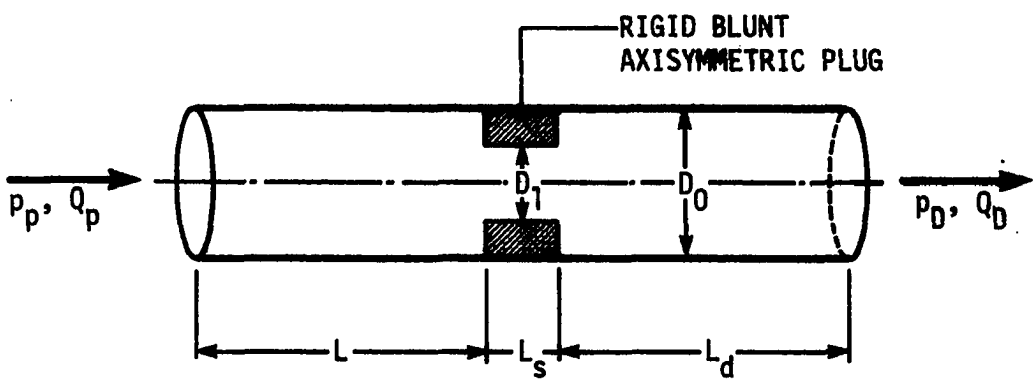
RIGID BLUNT AXISYMMETRIC PLUG
D_1
D_0
p_p, Q_p
p_D, Q_D
L
L_s
L_d

1. The cross-sectional area of the tube is a linear function of the pressure and changes in the area are small compared to some reference area.
2. The friction term in the axial momentum equation can be approximated by the Poiseuille flow friction term.
3. The convective acceleration term in the momentum equation can be neglected.
4. The tube is taken to be nontapered, homogeneous, and incompressible.

The linearized continuity and axial momentum equations can then be written as

$$\frac{\partial Q}{\partial x} + C \frac{\partial p}{\partial t} = 0 \tag{3.1}$$

and

$$\frac{\partial p}{\partial x} + RQ + L \frac{\partial Q}{\partial t} = 0 \tag{3.2}$$

where $R = 8\pi\mu/A_0^2$ and $L = \rho/A_0$.

Stenosis Model

The following empirical equation derived by Young and Tsai (1973a,b) is used to obtain the pressure drop across a rigid constriction in a flexible tube.

$$\Delta p = \frac{4K_v\mu}{\pi D_0^3} Q + \frac{8K_t\rho}{\pi^2 D_0^4} \left(\frac{A_0}{A_1} - 1\right)^2 |Q|Q + \frac{4K_u\rho L_s}{\pi D_0^2} \frac{dQ}{dt} \tag{3.3}$$

The coefficients K_t, K_u and K_v generally depend upon the stenosis geometry and the frequency parameter. Of these, K_t and K_u appear to exhibit only slight dependence on the geometry and the frequency parameter. Their values can be approximated by 1.52 and 1.2, respectively, for

simple stenosis geometries (Young and Tsai, 1973a,b). The authors also suggest that K_v can be approximated by the equation

$$K_v = 32 \frac{L_a}{D_0} \left(\frac{A_0}{A_1}\right)^2 \tag{3.4}$$

where

$$L_a = 0.83L_s + 1.64D_1 \tag{3.5}$$

Numerical Solution

The finite element method was used to solve the system of partial differential equations. The solution domain was discretized in time and in the axial direction by using linear rectangular elements. The discretization scheme is illustrated in Fig. 3.2. The horizontal and vertical sides of each element represent a length and time step, respectively. A coordinate system embedded in the centroid of each element was used. Based on this coordinate system, the nondimensional spatial and time variables could be defined as follows:

$$r = x/a \tag{3.6}$$

and

$$s = t/b \tag{3.7}$$

where a and b are the half length and time steps, respectively. Nodal pressures and flows were described by the equation

$$\begin{Bmatrix} P \\ Q \end{Bmatrix} = [N]\{\delta\}_e \tag{3.8}$$

where [N] is the shape function matrix given by

$$[N] = \begin{bmatrix} N_1 \\ N_2 \end{bmatrix} = \begin{bmatrix} N_1, 0, N_2, 0, N_3, 0, N_4, 0 \\ 0, N_1, 0, N_2, 0, N_3, 0, N_4 \end{bmatrix}$$

Fig. 3.2. Details of finite element grid showing time and spatial coordinate system

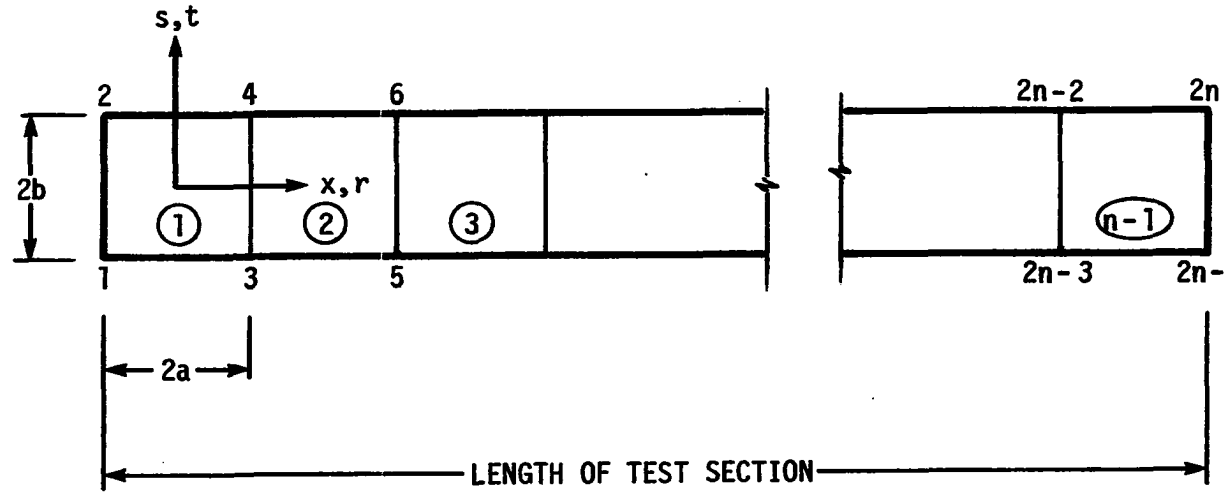
s,t
2
4
6
2n-2
2n
2b
x,r
1
2
3
n-1
1
3
5
2n-3
2n-1
2a
LENGTH OF TEST SECTION

with

$$N_i = (1/4)\ (1 + rr_i)(1 + ss_i)$$

$$r_i = \pm 1, \quad s_i = \pm 1, \quad i = 1, 2, 3, 4$$

$$\{\delta\}_e = [p_1, Q_1, p_2, Q_2, p_3, Q_3, p_4, Q_4]^T$$

The nodal pressure and flow equation was substituted into Eqs. (3.1) and (3.2) to obtain

$$L_1 = [N^2]_r r_x \{\delta\}_e + C[N^1]_s s_t \{\delta\}_e \tag{3.9}$$

and

$$L_2 = \frac{\rho}{A_0}[N^2]_s s_t \{\delta\}_e + [N^1]_r r_x \{\delta\}_e + \frac{8\pi\mu}{A_0^2}[N^1]\{\delta\}_e \tag{3.10}$$

where $[N^2]_r = \partial[N^2]/\partial r$, $r_x = \partial r/\partial x$, etc. The Galerkin method was used to obtain the element equations,

$$\int_A ab[N]^T L_1 dA + \int_A ab[N]^T L_2 dA = 0 \tag{3.11}$$

where $dA = dsdr$. The element equations were assembled using the direct assembly procedure to obtain the global equation given by

$$[A]\{\delta\} = 0 \tag{3.12}$$

where [A] is a 2n by 2n matrix of constant coefficients and

$$\{\delta\} = [p_1, Q_1, p_2, Q_2, \ldots, p_{2n}, Q_{2n}]^T$$

As the solution marches in time, the pressures and the flows at the odd numbered nodes are known from the solution at the previous time step. Thus, the number of unknowns is reduced by half the original number and the [A] matrix is now a n by n matrix. The known pressures and flows are multiplied by the corresponding coefficients in the [A] matrix and carried to the right hand side of Eq. (3.12) to form the force vector. Equation (3.11) is then written as

$$[A^*]\{\delta^*\} = \{f^*\} \tag{3.13}$$

where $[A^*]$ is the reduced [A] matrix, $\{f^*\}$ is the force vector and $\{\delta^*\}$ is given by

$$\{\delta^*\} = \{p_2, Q_2, p_4, Q_4, \ldots, p_{2n}, Q_{2n}\}^T$$

Equation (3.13) constitutes a set of algebraic equations describing the flow in an unobstructed tube.

The position of an isolated stenosis in the tube is specified by assigning an element number to it. The tube then consists of three parts, a portion of unobstructed tubing proximal and distal to the stenosed element and the stenosis element itself. The equations that govern the flow in the stenosed element are given by

$$p^K_{2m} - p^K_{2m+2} = \frac{4K_v}{\pi D^3} Q^K_{2m} + \frac{8K_t\rho}{\pi^2 D^4} \left(\frac{A_0}{A_1} - 1\right)^2 |Q^K_{2m}| Q^K_{2m} + \frac{K_u \rho L}{\pi D^2} \frac{Q^K_{2m} - Q^{K-1}_{2m}}{\Delta t} \tag{3.14}$$

and

$$Q^K_{2m} = Q^K_{2m+2} \tag{3.15}$$

where Δt is the time increment. The superscripts and the subscripts in Eqs. (3.14) and (3.15) refer to the time levels and to the node number, respectively.

Equations (3.13) through (3.15) constitute a set of algebraic equations describing flow through an obstructed tube. Proximal and distal boundary conditions need to be specified to solve this set of equations. In this study, the proximal flow and a lumped linear distal resistance were used as boundary conditions. This set of boundary conditions have previously yielded good results (Rooz, 1980). Additional details of development of the element and global coefficient matrix and the numerical solution procedure used in this study are given in Rooz (1980).

Parameter Estimation Technique

As noted elsewhere, the parameter estimation technique provides a means of indirectly estimating system parameters from directly measured system variables. The mathematical model used in this study contains several parameters which are of interest in a study of flow through a segment of obstructed artery. These are as follows: fluid density, fluid viscosity, vessel radius, vessel length and compliance, and parameters pertaining to the stenosis such as its severity and location. In addition, if the distal boundary condition is specified by prescribing a lumped linear resistance, then the distal resistance could be added to the parameters to be estimated. In this study, the fluid properties were assumed to be known since they can be readily measured directly. It was also assumed that the vessel length between the upstream and downstream measurement sites was known. The UET used to track the diameter changes could also be used to determine an approximate value for the vessel diameter (Mozersky et al., 1972; Hokanson et al., 1972). Also, the compliance of the latex tube used in the hydraulic model was calculated directly from the experimental data. The details of the compliance calculations are given in the Appendix. Thus, the system parameters to be estimated were the stenosis parameters, and the distal resistance (if used as a boundary condition).

The process of estimating the desired parameters involves the following steps:

1. Set the values of the unknown parameters in the model at an initial value, which is assumed.
2. Use measured values of the system variables as boundary conditions and solve the model.
3. Record the values of the pressures and flows at desired locations along the length of the tube as predicted by the model.
4. Compare the predicted value of the variable used for model fitting with the corresponding directly measured value.
5. Adjust the value of the model parameters systematically to minimize the difference between the measured value of the system variable and the corresponding value predicted by the model. The values of the parameters which minimize this difference are taken to be the best estimates for those parameters.

This process is depicted schematically in Fig. 3.3.

In this study, the method of ordinary least squares (OLS) was used to obtain the optimum estimates for the parameters. In this method, an attempt is made to minimize the value of the sum of the squares of the difference between the measured value of a variable and the corresponding value predicted by the model. Thus, if

$$S = [\bar{Y} - \bar{y}(\bar{b})]^T[\bar{Y} - \bar{y}(\bar{b})] \tag{3.16}$$

where

$\bar{Y}$ = a set of measured values

$\bar{y}(\bar{b})$ = corresponding model values for a set of parameters $\bar{b}$

Then, in the OLS scheme, an attempt is made to minimize the value of S by varying the values of the system parameters.

Fig. 3.3. Schematic representation of parameter estimation scheme

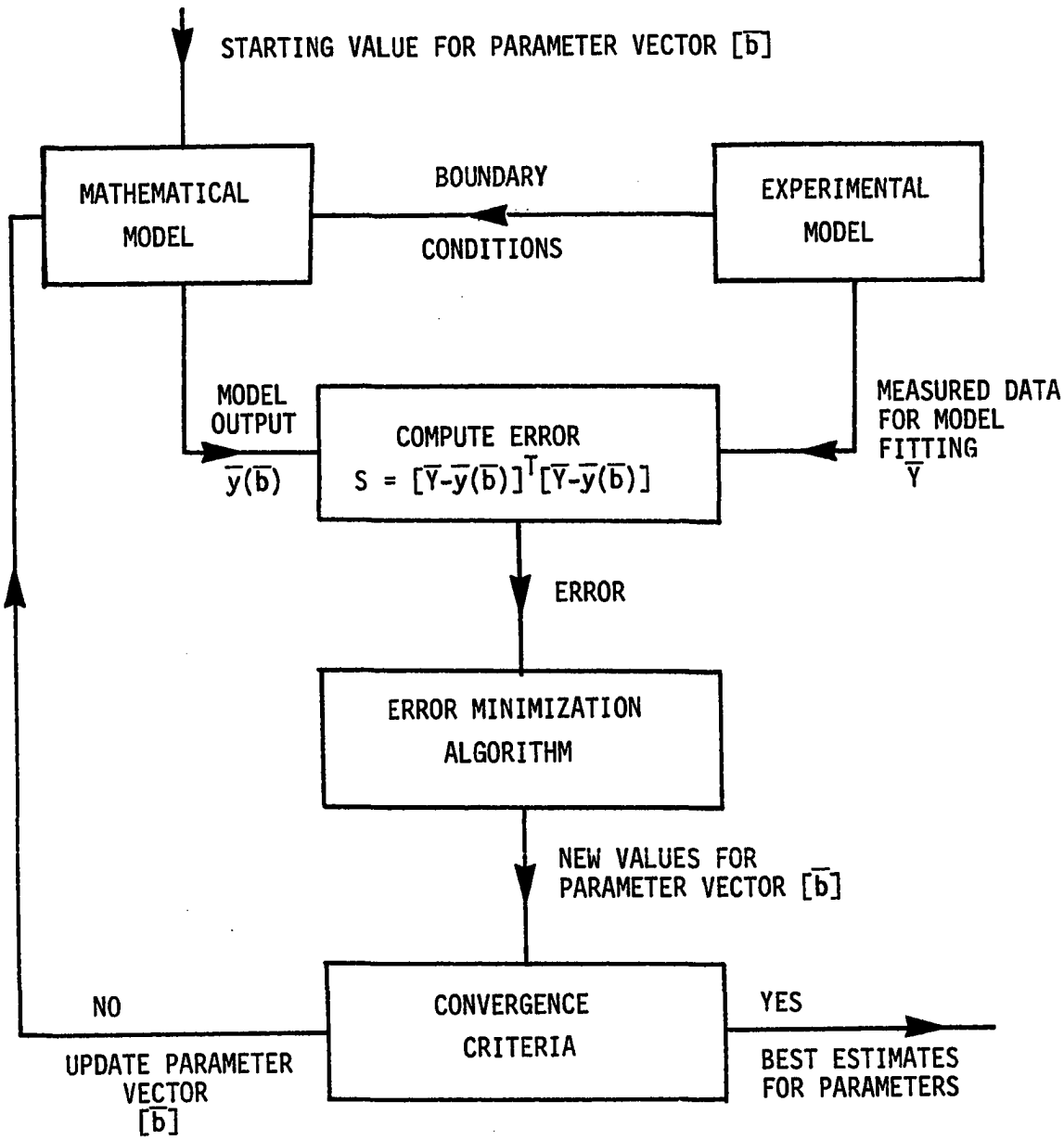
STARTING VALUE FOR PARAMETER VECTOR [b̄]
MATHEMATICAL MODEL
BOUNDARY CONDITIONS
EXPERIMENTAL MODEL
MODEL OUTPUT
ȳ(b̄)
COMPUTE ERROR
S = [Ȳ-ȳ(b̄)]ᵀ[Ȳ-ȳ(b̄)]
MEASURED DATA FOR MODEL FITTING
Ȳ
ERROR
ERROR MINIMIZATION ALGORITHM
NEW VALUES FOR PARAMETER VECTOR [b̄]
CONVERGENCE CRITERIA
NO
UPDATE PARAMETER VECTOR [b̄]
YES
BEST ESTIMATES FOR PARAMETERS

In general, $\bar{y}(\bar{b})$ can be linear or nonlinear in the parameters. For the problem being studied, $\bar{y}(\bar{b})$ is a nonlinear function of $\bar{b}$. The Gauss-Newton linearization scheme (Beck and Arnold, 1977) has been used in this study to linearize the minimization scheme. Details of the linearization scheme can be found in Gray (1981). This method yields an interative scheme of the form given by Eq. (3.17) to update the values of the vector and minimize the value of S through the equation.

$$\bar{b}^{K+1} \approx \bar{b}^{K} + ([X^{K}]^{T}[X^{K}])^{-1}([X^{K}][\bar{Y} - \bar{y}]) \tag{3.17}$$

where

$\bar{b}^{K}$ = the vector of parameter values at the kth iteration

$[X^{K}]$ = the sensitivity matrix

$\bar{Y}$ = the vector representing measured data

$\bar{y}$ = the vector representing model corresponding model response

The superscripts in Eq. (3.17) refer to the iteration level.

The sensitivity coefficient matrix [X] in Eq. (3.17) is computed by using the Taylor series approximation. Initially, the model is solved using the parameter values $\{\bar{b}\}$. Next, the first component of b_1 of the vector is incremented by a small amount and all the other elements of the vector are kept at their initial values. The model is solved again and a first order approximation for the matrix [X] is computed by using Eq. (3.18), i.e.,

$$X^{K}_{ij} = \frac{\partial y^{K}_{i}}{\partial b_{j}} = \frac{y(t_i, b^{K}_{j} + \Delta b^{K}_{j}) - y(t_i, b^{K}_{j})}{\Delta b^{K}_{j}} \tag{3.18}$$

This process is repeated for all other parameters. The parameter vector $\bar{b}^{K+1}$ obtained by using Eq. (3.17) represents a better estimate for the

parameter values if the value of S in Eq. (3.16) decreases with each iteration.

Usually, computation is stopped when the change in the value of $\bar{b}^K$ is very small compared to $\bar{b}^K$, i.e., when

$$\Delta_1 b_j^{K+1} = \frac{|b_j^{k+1} - b_j^K|}{|b_j^K| + 10^{-30}} < 0.001 \quad j = 1, 2, 3, \ldots, n \tag{3.19}$$

It has been observed (Beck and Arnold, 1977) that the value of $\bar{b}^{K+1}$ that meets the criterion described by Eq. (3.19) may not yield a minimum for the value of S. It is, therefore, necessary to monitor the value of S at each iteration level. It has also been observed that the value of S may increase temporarily in order to reach a parameter space where a global minimum exists. It is noteworthy that $\Delta_1 b_j^{K+1}$ seems to decrease with a decrease in S in the parameter space where a global minimum for S exists. In this study, the values of $\Delta_1 b_j^{K+1}$ and S were monitored at each iteration level. Initially, the search for a new value of the vector $\bar{b}^{K+1}$ was carried out until the value of S started to increase. Or,

$$S^{K+1} > S^K$$

At this point, a test was performed to see how the term $\Delta_1 b_j^{K+1}$ was behaving. The following two cases were observed, and depending on the value of $\Delta_1 b_j^{K+1}$, the following action was taken.

Case 1

$$S^{K+1} > S^K$$

and

$$\Delta_1 b_j^{K+1} > \Delta_1 b_j^K$$

Search for a better value of $\bar{b}$.

Case 2

$$S^{K+1} > S^{K}$$

and

$$\Delta_1 b_j^{K+1} < \Delta_1 b_j^{K}$$

The value of the parameter vector was reinitialized to the value at previous iteration level K, and the step size in the parameter space was halved. The search was continued until the step size was reduced by 1/8 of its original value. Finally, the value of S when the solution converged was compared with the least value of S obtained during the solution procedure. If the value of S at convergence was the least value obtained, then the iteration procedure was terminated and the value of the parameter vector which gave this minimum value of S was taken to be the best estimates for the model parameters. Otherwise, the value of the parameter vector was reinitialized at the value which gave the least value of S through the iteration procedure, the step size for incrementing the parameters was reduced to half its starting value, and iterations restarted to see if a better minimum for S could be obtained. At the end of this procedure, the value of the parameter vector which yielded the minimum value of S was taken to be the best estimates for the model parameters.

One of the difficulties associated with the use of parameter estimation techniques is that they can yield nonunique results. In other words, there may be more than one combination of the parameter values which yield the same value of S. Also, the optimum estimates for $\{\bar{b}\}$ may depend on the initial guess for the value of the parameter vector $\{\bar{b}\}$. The

termination criterion outlined above seemed to alleviate the problems of nonunique estimates and starting value dependency, at least for the problem under investigation.

CHAPTER 4. EXPERIMENTAL METHODS AND MATERIALS

A major objective of the present study was to determine the feasibility of using noninvasively measured values of the system variables to estimate certain unknown parameters in the system. It was, therefore, necessary to build a simple physical model from which direct measurements of parameters could be obtained to compare them with the estimated values. In a physical model, it is possible to measure the system variables fairly simply and accurately, and also vary the system parameters, such as the compliance of the tube, and the severity and the location of the stenoses. Once the measurement techniques and the efficacy of the estimation scheme were validated in a simple model, they could be applied to a more complex physiological system. The physical model used in this study consisted of a hydraulic model of pulsatile flow in a flexible tube containing an obstruction.

The hydraulic model was used for the following purposes:

1. To explore the feasibility of using the UET to predict pressure waveforms and vessel compliance.
2. To compare the estimates for the compliance of the tube and the stenosis parameters obtained by using noninvasive measurements with those obtained by using invasive measurements. The estimated values were also compared with the values measured directly from the hydraulic model.

To further validate the technique, animal experiments were conducted on mongrel dogs. Details of the hydraulic model and animal experiments are given in this chapter.

Hydraulic Model

The main components of the model consist of a flexible tube, a variable speed and discharge pump, and a distal resistance in the form of a series of small diameter tubes stretched in parallel between two headers. The data acquisition system consisted of a Grass model 7 polygraph, which was used to record the analog signals received from Statham pressure transducers (P23Dc), the ultrasonic echo tracking system (D. E. Hokanson, Inc.), the electromagnetic flowmeter (Biotronix BL-610) and a Parks model 909 continuous-wave Doppler flowmeter. The analog signal received by the strip chart recorder was sampled every 0.010 s and digitized by using an eight channel A/D converter and the digitized data were acquired by an eight bit CBM model 2001 PET microcomputer and stored on floppy diskettes for further analysis. Figure 4.1A shows the pump, the flexible tube test section, the distal resistance and the instrumentation used in the hydraulic model testing. Figure 4.1B shows a general layout of the laboratory and the data acquisition and storage systems. Details of the test section and distal resistance used can be seen in Figures 4.2A and 4.2B, respectively.

A flexible latex tube (6.34 mm I.D.) was used to simulate the artery. The ends of the tube were attached to Plexiglas fittings which were fixed to the test bench. This arrangement prevented the axial movement of the tube but allowed it to expand and contract in the radial direction. Hypodermic needles were introduced into the Plexiglas fittings through holes drilled in them. The position of the needles were adjusted

Fig. 4.1A. General layout of the hydraulic model
P = variable speed, variable discharge pump
FTTS = flexible tube test section
DR = distal resistance
FM = electromagnetic flowmeter
EC = phase-locked echo tracker
UF = continuous-wave Doppler flowmeter
W = water column

Fig. 4.1B. General layout of hydraulic model showing details of data acquisition system

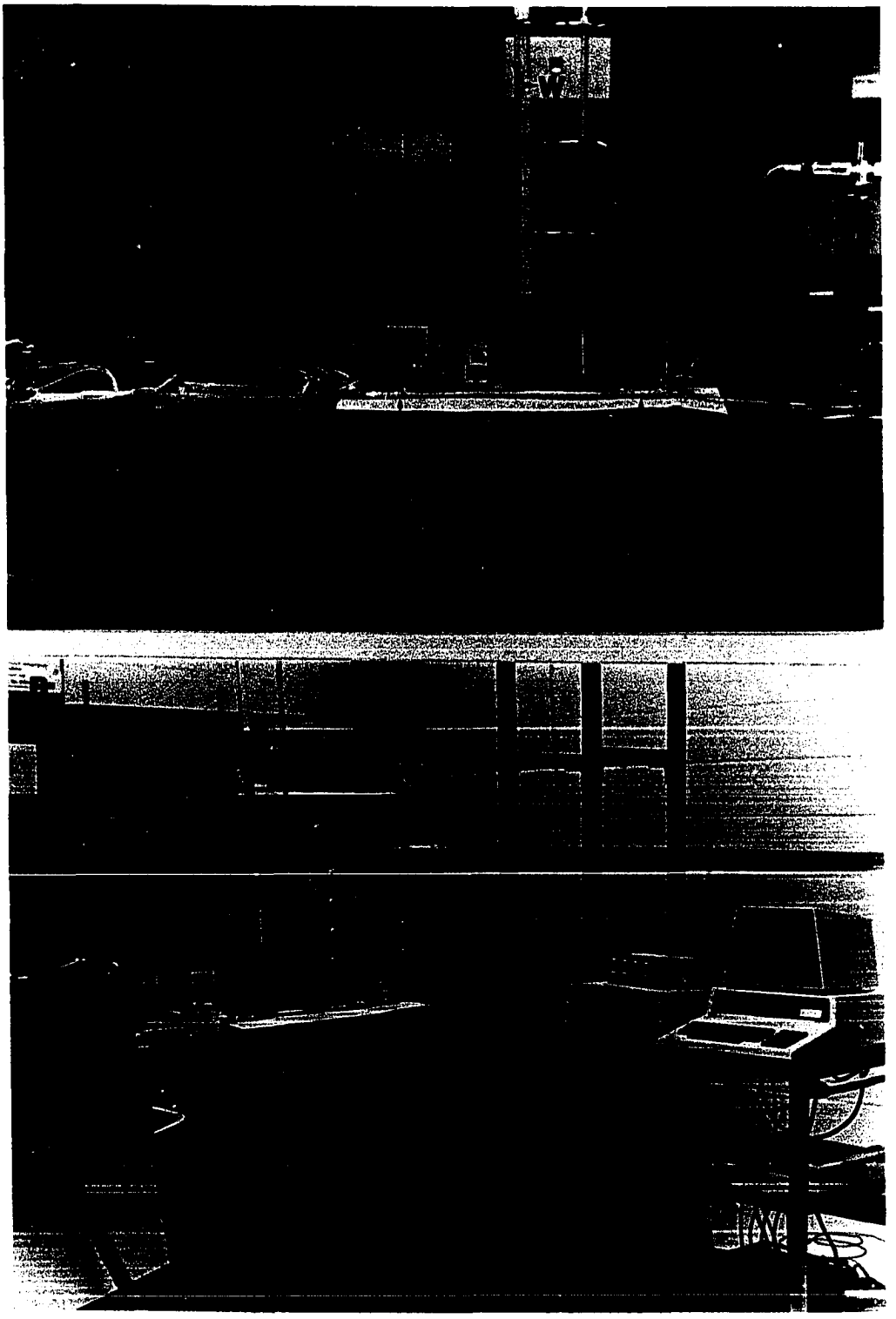

Fig. 4.2A. Details of hydraulic model showing invasive instrumentation
WL = working length of flexible tube
S = stenosis
PFP = proximal electromagnetic flow probe
DFP = distal electromagnetic flow probe
PPT = proximal pressure transducer
DPT = distal pressure transducer

Fig. 4.2B. Details of distal resistance

Fig. 4.2C. Details of arrangement to constrain axial movement of flexible tube showing pressure transducer

Fig. 4.2D. Middle section of test section showing Plexiglas plugs used to simulate stenoses

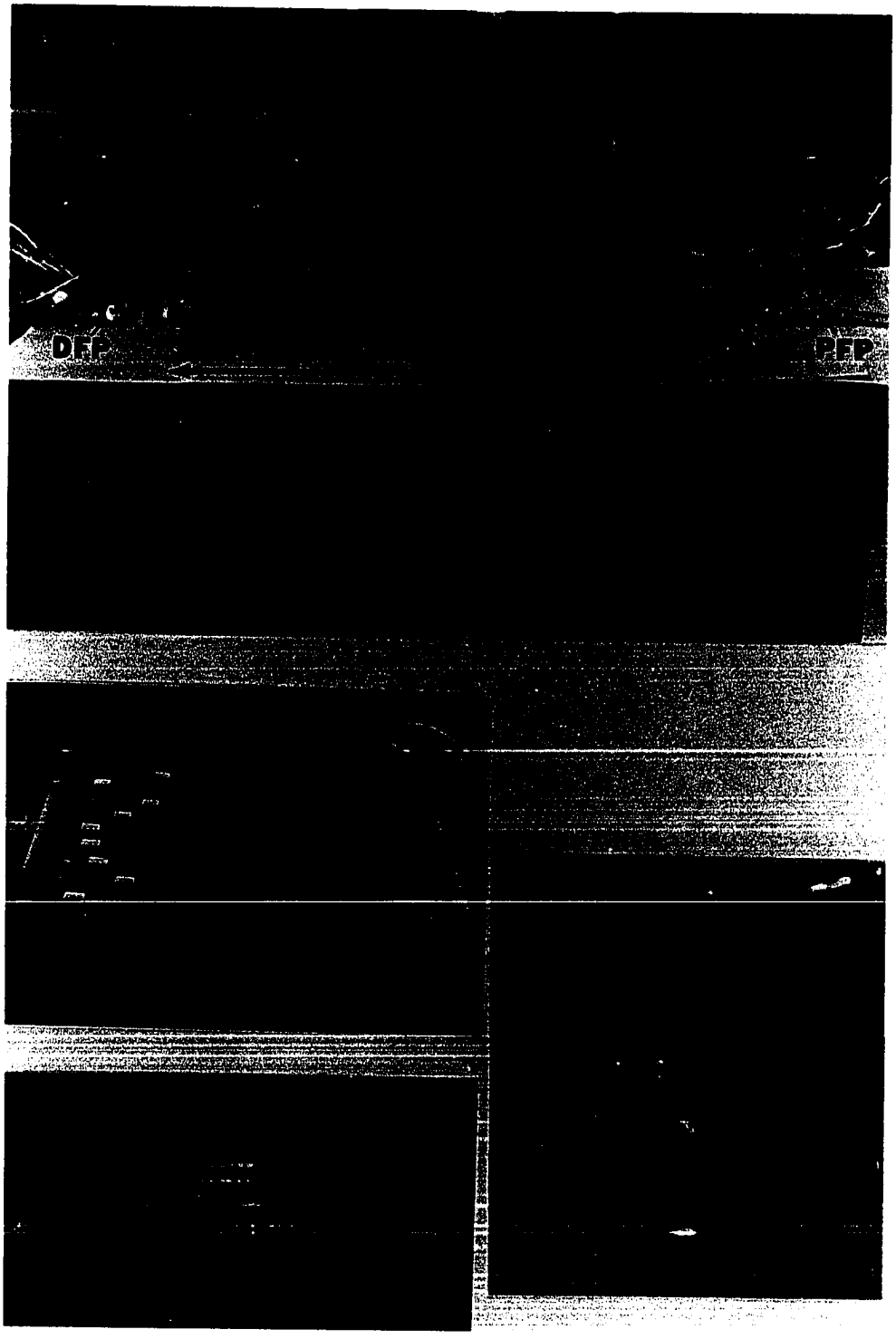
DFP
CFP

such that their ends were flush with the inside walls of the fittings and did not disturb the flow. Strain gauge type pressure transducers were connected to the outer ends of the hypodermic needles to measure the pressures at both the proximal and distal ends of the tube. Flow in the tube was measured by two 3-mm lumen diameter, in-line electromagnetic flow probes (In-Vivo Metric), mounted in close proximity to the pressure taps. The flow probes were connected to an electromagnetic flowmeter. This arrangement made up the instrumentation for invasive pressure and flow measurements. Figure 4.2A shows the test section of the latex tube and the arrangement of the proximal and distal pressure transducers and electromagnetic flowmeters. Figure 4.2C shows the details of arrangement to constrain the axial movement of the test section and Fig. 4.2D shows the stenosis.

A Parks model 909 continuous-wave Doppler flowmeter was used to measure the flow in the tube noninvasively. A flow probe holder was designed and fabricated to allow the probe to be pivoted through an angle of 45° from its initial position. The probe was initially positioned such that its axis was perpendicular to the axis of the tube. It was then rotated through an angle of 45° to measure the flow. Figures 4.3A and 4.3B show details of the positioning of the USF.

The phase-locked echo tracking system (UET) used in this study was developed by Hokanson et al. (1972) specifically to measure transcutaneously the diameter of an artery and the diameter changes that occur with the pressure pulse in major peripheral arteries. A transmitter is used to transmit repeated short bursts of ultrasound of approximately 5 MHz towards the artery and to detect the echo from the artery. The time

Figs. 4.3A and 4.3B. Details of ultrasonic flow probe positioning

Figs. 4.3C and 4.3D. Details of echo-tracker probe positioning

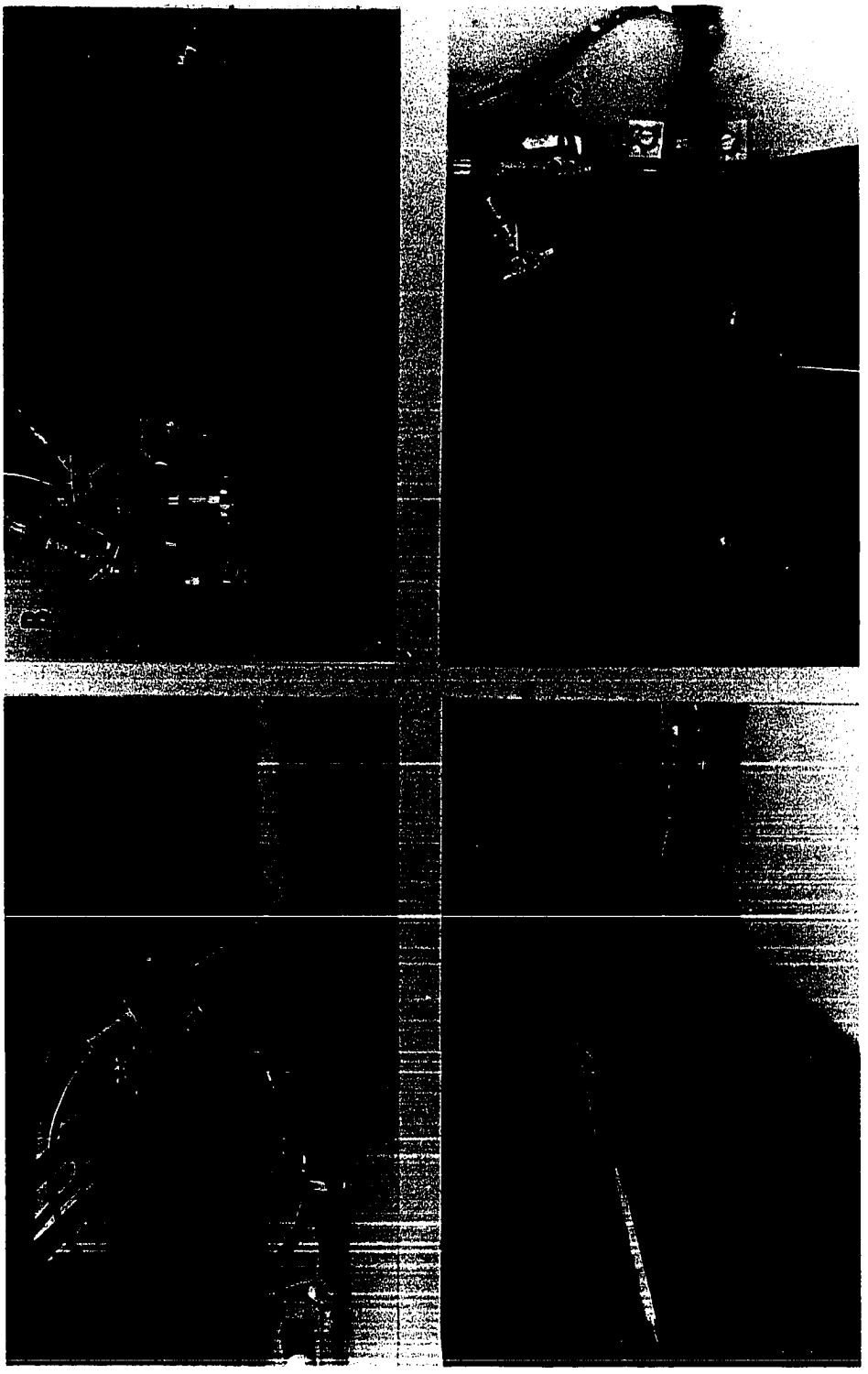

interval between the transmission of the ultrasound burst and its reception depends on the distance from the transmitter to the reflecting surface. The output of the receiver is displayed on an oscilloscope synchronized with the repetition rate of the transmitter to permit the observation of the moving echoes caused by the displacement of the arterial wall. The oscilloscope is also used to show the position of two tracking gates in relation to the moving echoes. When these gates are moved to coincide with the position of the echoes and locked on to them, they will follow the moving echoes. The distance between the tracking gates is converted into a voltage which is amplified and fed to the recording device (Grass model 7 polygraph) to measure the changes in the diameter of the artery. This system is capable of measuring diameter changes of the order of 0.002 mm while the diameter of the artery can be measured to within 0.1 mm.

The UET probe was mounted vertically on a positioning stand which was clamped to the test bench. The probe was positioned on the test section of the tube some distance away from the fixed ends, and the echoes from the tube were monitored on an oscilloscope. The probe was positioned such that it was perpendicular to the axis of the tube and the echoes from the walls of the tube were sharp. Figures 4.3C and 4.3D show the details of the positioning of the UET.

The test fluid was a solution of potato starch in physiological saline. The density and the viscosity of the solution were 997 kg/m^3 and 0.89 $mN\text{-}s/m^2$, respectively. Pulsatile flow was produced by a variable stroke syringe pump powered by a variable speed motor. A closed loop flow

system was used in which the pump took suction from a closed reservoir. The pump discharge was connected to the test section through a length of clear plastic tubing. The discharge from the test section passed through the distal resistance from where it returned to the closed reservoir.

Calibration of Instruments

Pressure transducer calibration

The pressure transducers were calibrated by pressurizing the flow system through a series of pressures and reading the corresponding values of pressure head directly from a water column. Simultaneously, the voltage signal from the pressure transducer was recorded on the strip chart recorder, digitized and stored on floppy diskettes for further analysis.

Ultrasonic echo tracker calibration

The UET was calibrated by using a calibration device built into the echo tracker. When the calibration button on the UET was pressed, the voltage output from the instrument corresponded to a distance of 5 mm. The instrument output was first zeroed and the corresponding deflection in the strip chart recorder was digitized and stored. Next, the calibration button was pressed and the deflection on the strip chart recorder was digitized and stored for further analysis. It is worth noting that the calibration signal of the UET corresponded to a distance of 5 mm. This was very large compared to the maximum diameter change in the tube which was of the order of 0.5 mm for the pressures generated by the pump. Care

had to be taken in adjusting the settings of the recorder to avoid saturating the amplifiers at the calibration signal.

Flowmeter calibration

The electromagnetic and ultrasonic flowmeters were calibrated under steady-flow conditions. At the end of each experimental run, the pump was stopped and the flow system connected to a calibration reservoir containing the test solution. The calibration reservoir was placed approximately one meter above the test bench. Under steady-flow conditions, a quantity of the fluid flowing through the system was drawn into a graduated cylinder. The time taken to collect the fluid was also noted. The volume of fluid collected when divided by the time taken gave the flow rate. The signal received from the flowmeters corresponding to each flow rate was digitized and stored for analysis. Typically, five sets of data each were collected and stored to calibrate the flowmeters and the pressure transducers.

Experimental Procedure

The experimental setup described above was first used to validate the use of the UET and then to acquire both invasive and noninvasive pressure and flow data for use in the parameter estimation scheme. The details of the experimental procedure are given below.

Verification of the UET

A series of dynamic tests were carried out on two latex tubes of different wall thicknesses to evaluate the performance of the UET. Each tube had an I.D. of 6.34 mm and was 0.39 m long. The tube was straight

and unobstructed. At the start of each test, the pump was started and left running until steady flow was achieved. The UET probe was positioned some distance from the fixed ends of the tube and acoustically coupled to the wall of the tube through a gel. The reflections from the walls of the tube were monitored on an oscilloscope and the gates of the UET were set to track the motion of the walls of the tube as the fluid flowed through it. The output from the UET and the pressure transducer nearest to it were recorded on the strip chart recorder, digitized and stored for analysis. The output from the UET when recorded gave the contour of the arterial wall-displacement pulse. The output from the pressure transducer gave the contour of the instantaneous pressure pulse. In each test, data corresponding to three cycles of pulsatile flow were recorded and stored for analysis. The pump was then stopped and the UET and the pressure transducer were calibrated as described. An analysis and calibration program written in CBM Basic was used to analyze the raw data from each test and to calculate the compliance of the tube using the formula

$$C = \frac{\pi D_{mean}(D_{max} - D_{min})}{2(p_{max} - p_{min})} \qquad (4.1)$$

where

C = compliance of the tube

D_{max} = maximum diameter of the tube in a cycle

D_{min} = minimum diameter of the tube in a cycle

D_{mean} = diameter of the tube at atmospheric pressure

p_{max} = maximum pressure in a cycle

p_{min} = minimum pressure in a cycle

The details of the calculation of the compliance are given in the Appendix. The calibration program was also used to convert the arterial wall-displacement waveform into the instantaneous pressure pulse.

Each dynamic test was followed by a static test to determine the compliance of the tube directly. The tube was clamped off upstream of the proximal pressure tap and downstream of the distal pressure tap. The distal pressure transducer was disconnected and known volumes of the test fluid were injected in incremental steps into the test section. The rise in pressure corresponding to each incremental volume injected was noted. The incremental volume at each step was divided by the length of the test section to obtain the increase in cross-sectional area of the tube at each step. The increment in area was plotted against the pressure in the tube, and the slope of this curve, dA/dP gave the compliance of the tube.

Tests with stenoses

Blunt Plexiglas plugs with outside diameter of 6.34 mm and specified inner diameters were used to simulate stenoses of varying severities. Figure 4.2D shows the midsection of the latex tube and some of the plugs used to simulate the stenoses. In each experimental run involving a stenosis, a plug of known internal diameter was inserted into the tube so that it formed an axisymmetric constriction in the flow field. The plug was placed midway between the proximal and distal measurement sites and its position fixed by using an external tie. The pump was started and run until steady flow was reached. Data from the proximal and distal pressure transducers and flowprobes were recorded to obtain invasive measurements. The UET probe was first positioned near the proximal pressure tap and the

USF probe near the distal pressure tap such that the stenosis was located midway between these measurement points also. Initially, the USF probe was placed with its axis perpendicular to the axis of the tube. Then it was rotated so that its axis made an angle of 45° to the axis of the tube. The data from the USF corresponding to distal flow and the UET corresponding to proximal pressure were recorded, digitized and stored. The UET was calibrated in position. The position of the USF and the UET was interchanged with the pump still running and distal pressure and proximal flow data were recorded, digitized and stored. The UET was calibrated again in the new position. The pump was stopped and the USF and the EMF were calibrated under steady-flow conditions. Finally, the pressure transducers were calibrated. This completed one test run.

The seemingly complicated method of collecting noninvasive pressure and flow data was necessary since only one UET and one USF were available in the laboratory. If a pair of UETs and USFs were available, then the USF and UET probes could have been positioned at the proximal and distal measurement sites and the switching of the probes could have been avoided.

At the end of each test run, all the data were analyzed and a print-out of the flows and pressures over one cycle was obtained. The data from the UET were used to determine the compliance of the tube. A Fourier analysis program was used to calculate the Fourier coefficients which in turn were used to represent the pressure and flow waveforms. The Fourier coefficients and the compliance value obtained from each run were utilized as inputs into the parameter estimation program. For a subsequent test run, a plug of a different inner diameter was inserted into the tube and

the above procedure repeated. Tests were run with plugs which represented 94.3%, 86.0%, 74.8% and 53.8% area reductions.

Animal experiments

The aim of the animal experiments was to obtain invasive pressure and flow data from the femoral arteries of dogs after an isolated stenosis of known severity had been introduced into the artery. In each case, the pressure and flow proximal and distal to the stenosis were measured. These data were used as input into the parameter estimation scheme to estimate the stenosis parameters, and the estimated values compared with the measured experimental values. Figure 4.4A shows the general layout of the instrumentation used and Figure 4.4B shows the Grass polygraph used to record the analog signals and the data aquisition system.

Five mongrel dogs of either sex and weighing between 30 to 40 kg were anesthetized with sodium pentobarbitol (30 mg/kg) given intravenously. The left or the right femoral artery was exposed and prepared for catheterization. Stiff, thin walled pressure catheters filled with saline were introduced into two branches of the artery of inner diameters varying from 4.0 mm to 5.5 mm, and separated by distances varying from 50 mm to 70 mm. The tips of the catheters were flush with the vessel wall and did not disturb the flow. The circumference of the artery was measured by wrapping a piece of string four times around the vessel. The length of the string required when divided by four gave the circumference of the vessel. From this, the inner diameter of the vessel was calculated assuming that the vessel wall thickness was 13% of the outer diameter of the vessel. The artery was clamped off proximally and distally using

Fig. 4.4A. Details of laboratory setup for animal experiments showing instrumentation
FM = electromagnetic flow meter
P Tr = proximal and distal pressure transducers
PT = proximal and distal pressure cannulae

Fig. 4.4B. Details of data acquisition system for animal experiments

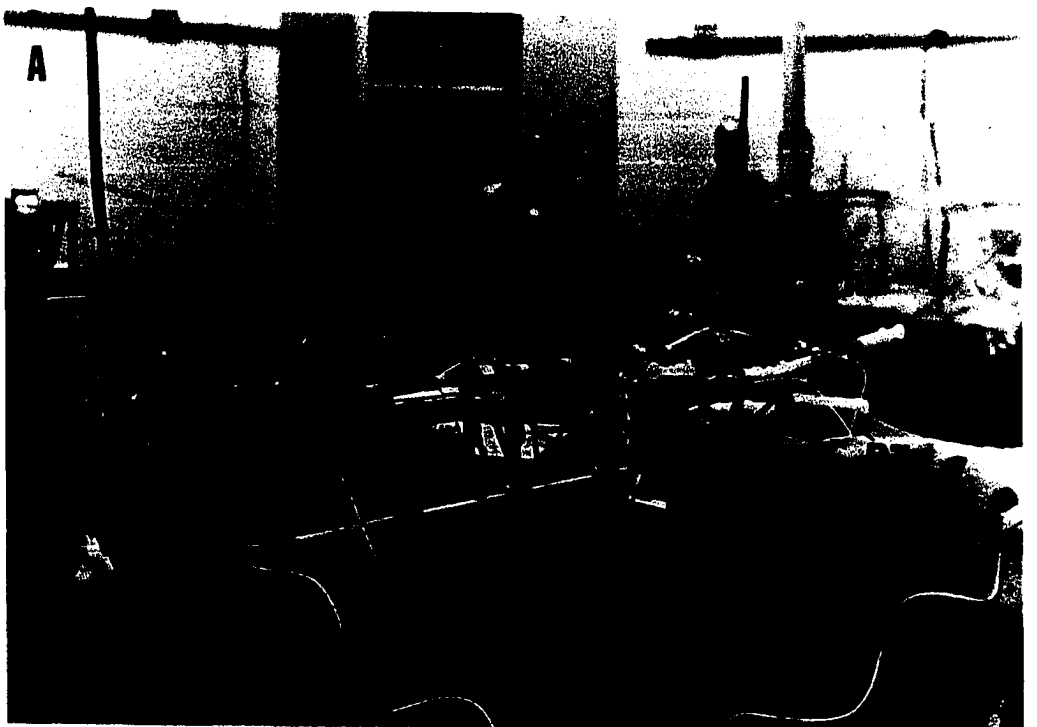
A

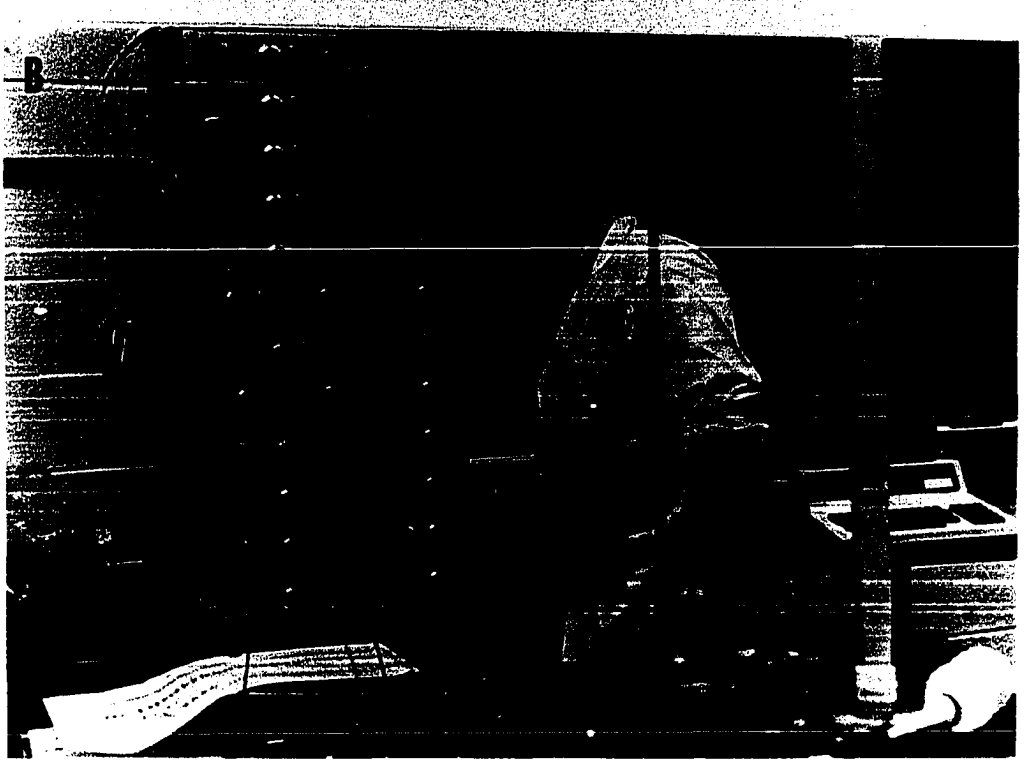
B

bulldog clamps. A blunt hollow Plexiglas plug with an external diameter approximately equal to inner diameter of the vessel was introduced midway between the pressure taps. Its position was fixed by using external ties. This plug simulated an isolated stenosis of known severity. The clamps were removed and two (In Vivo Metric) cuff type flow probes were mounted in close proximity to the pressure measurement sites. Figure 4.5A shows the exposed femoral artery and the position of the proximal and distal pressure transducers and electromagnetic flowmeters before the insertion of the stenosis, and Figure 4.5B shows the test section with the stenosis and the instrumentation in place. The animal was allowed to rest for a period of 10 minutes to allow the system to resume steady-state operation. Then, the proximal and distal pressure and flow data were collected over three heart cycles, digitized and stored. The length of the artery between the pressure measurement sites, the distance between the leading edge of the stenosis and the proximal pressure tap, the length and the inner and outer diameter of the stenosis and the heart rate were also recorded.

After the data had been collected, the flow meters were calibrated in vivo by collecting a measured quantity of blood over a known period of time. The animal was then euthanized. The pressure transducers were calibrated by using static calibration procedures outlined elsewhere. The data were analyzed and the Fourier coefficients were calculated to represent the proximal and distal pressures and flows. The Fourier coefficients and other required data were subsequently used in the parameter estimation scheme to estimate the stenosis parameters.

Fig. 4.5A. Details of animal experiments showing exposed femoral artery and invasive instrumentation prior to the insertion of stenosis
PT = proximal and distal pressure cannulae
PF = proximal and distal electromagnetic flow probes

Fig. 4.5B. Details of animal experiments showing exposed femoral artery with stenosis in place
PT = proximal and distal pressure cannulae
PF = proximal and distal electromagnetic flow probes
S = stenosis

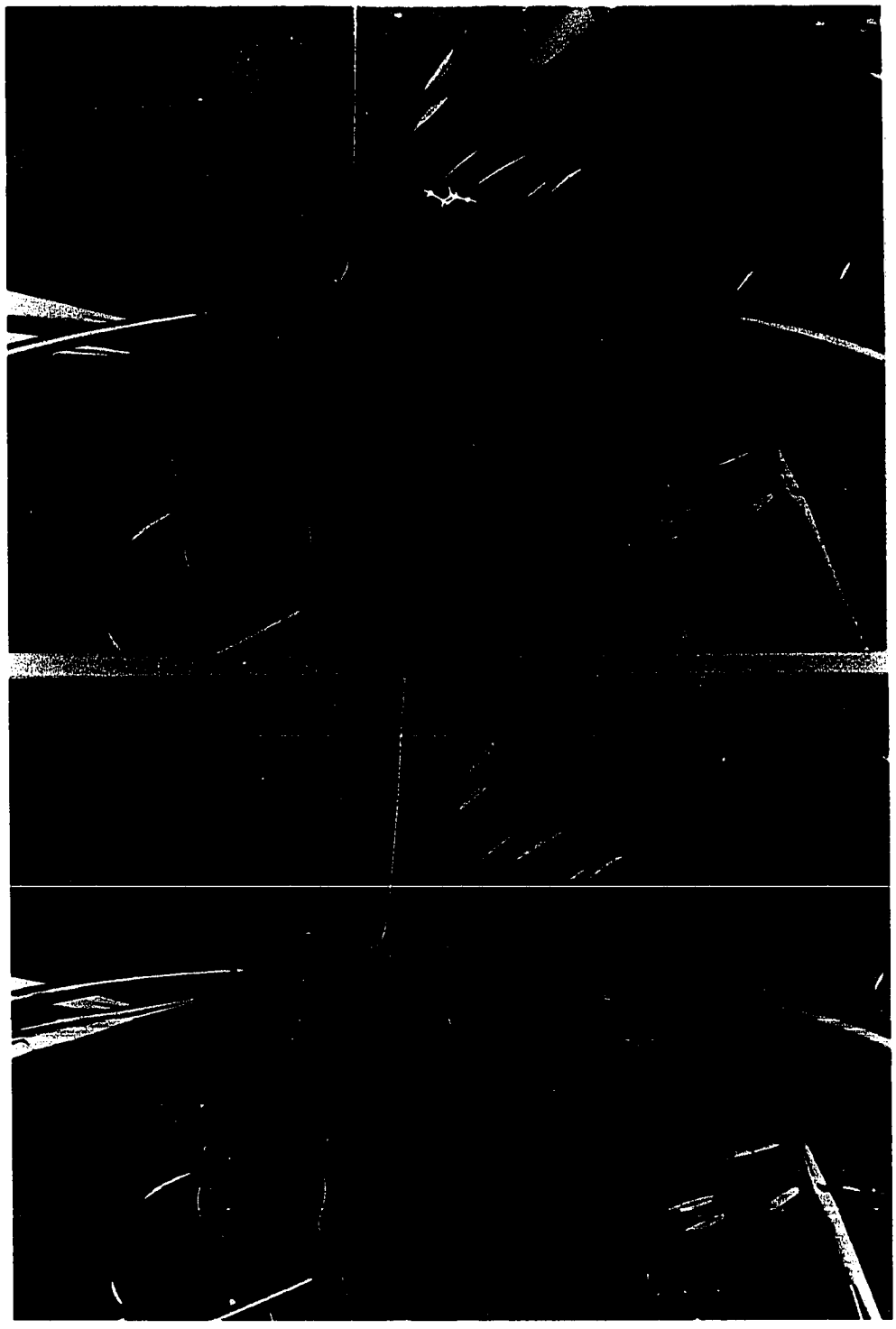

CHAPTER 5. RESULTS

The presentation of results of this study will be divided into five parts as follows:

1. The feasibility of using the UET to measure the linear compliance of a vessel and pressure waveforms is established.
2. The general validity of the parameter estimation technique is demonstrated by conducting model-to-model tests, in which computer model generated data are used as input to estimate the model parameters.
3. The use of noninvasive measurements as input to estimate system parameters in an unobstructed tube is considered.
4. The estimation of stenosis characteristics, based on noninvasive measurements is validated by comparing the estimates with measured experimental values. Estimates based on noninvasive measurements are also compared with those based on invasive measurements of the system variables.
5. The use of the estimation scheme in a physiological situation is investigated through animal experiments.

Measurement of Compliance with the UET

In this part of the study, the UET was used to determine the compliance of the latex tubes through a series of dynamic tests. Each dynamic test was followed by a static test to determine the compliance by direct measurement by the procedure outlined in the preceding chapter. The data from the direct compliance measurement tests are plotted in Figs.

5.1 and 5.2. The plots of the increase in the cross-sectional area of the tube against the pressure indicate that it is reasonable to assume a linear area-pressure relationship for the tubes used in the hydraulic model. A summary of the compliance measurement tests are given in Tables 5.1 and 5.2. It can be seen that the compliance predicted by the UET compares well with that measured directly.

The diameter-change waveform measured by the UET was transformed into a pressure pulse waveform by assuming a linear cross-sectional area-pressure relationship. The actual pressure waveform was measured simultaneously using the strain-gauge type pressure transducers. The test data were analyzed and the Fourier coefficients for the pressure waveforms were obtained. The pressure waveform measured directly and that obtained by transforming the UET data were then reconstituted by using the first five Fourier coefficients. One pair of reconstituted waveforms is shown in Fig. 5.3. It can be seen that the pressure waveform predicted by the UET compares well in phase and amplitude with that measured directly. The results of all other dynamic tests yielded similar correlations between the directly and indirectly measured pressure waveforms.

Validation of the Parameter Estimation Scheme

Rooz (1980) conducted experiments on a hydraulic model similar to the one used in this study to validate the mathematical model and the numerical solution scheme proposed by him. The results of this study showed very good agreement between the model predictions and experimental waveforms. Since the model and the numerical solution scheme used in this

Fig. 5.1. Change in cross-sectional area versus change in pressure for latex tube #1

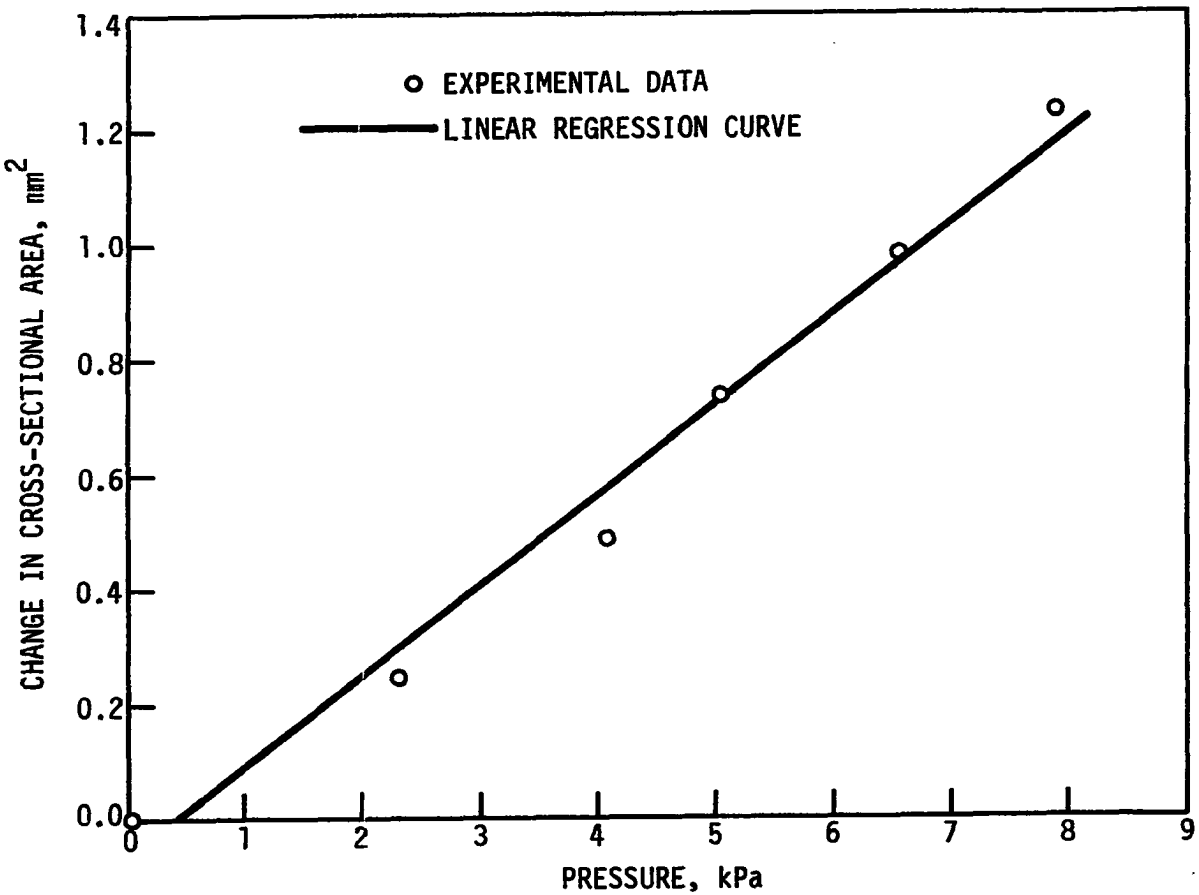
EXPERIMENTAL DATA
LINEAR REGRESSION CURVE
CHANGE IN CROSS-SECTIONAL AREA, mm2
PRESSURE, kPa
0.0
0.2
0.4
0.6
0.8
1.0
1.2
1.4
0
1
2
3
4
5
6
7
8
9

Fig. 5.2. Change in cross-sectional area versus change in pressure for latex tube #2

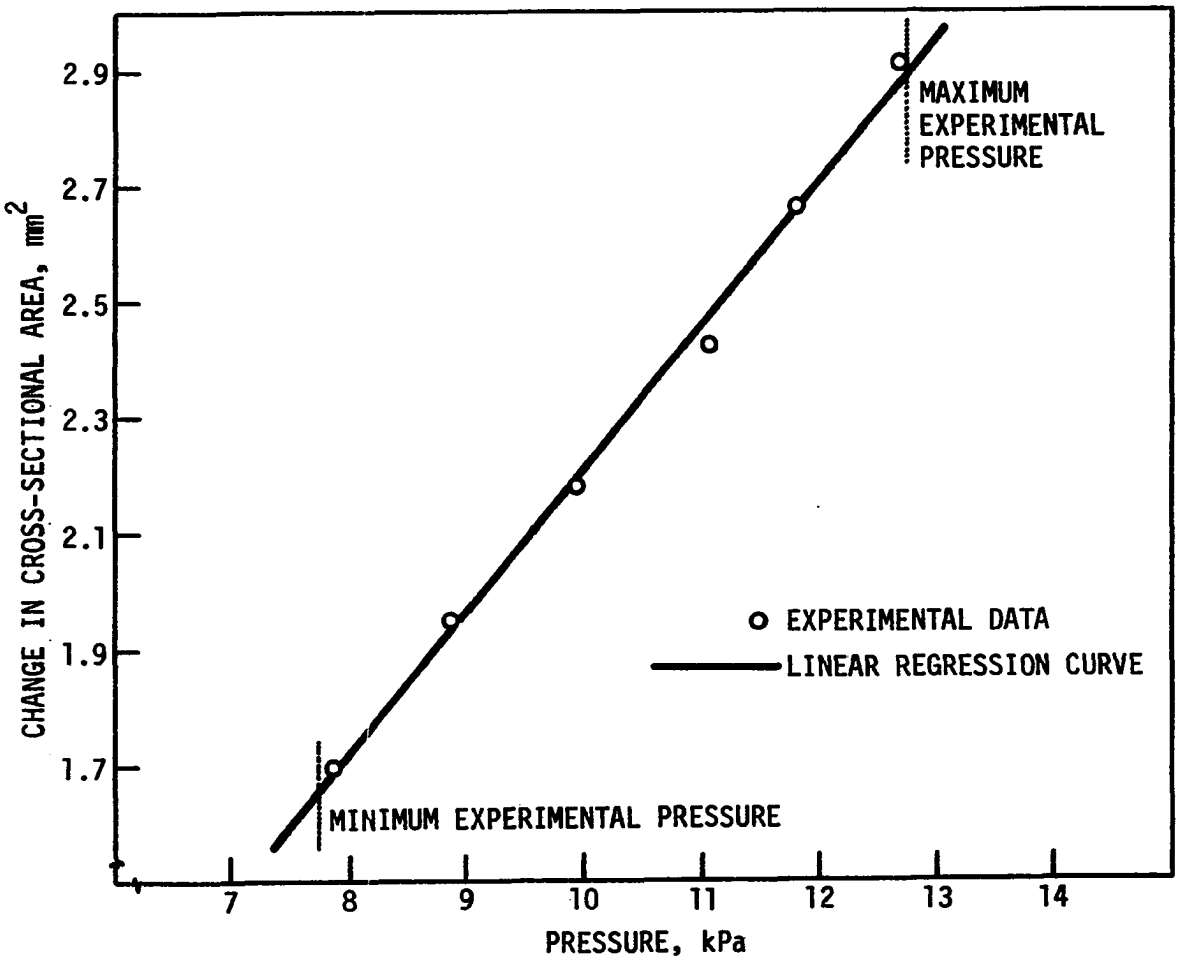
CHANGE IN CROSS-SECTIONAL AREA, mm²
2.9
2.7
2.5
2.3
2.1
1.9
1.7
7
8
9
10
11
12
13
14
PRESSURE, kPa
MAXIMUM EXPERIMENTAL PRESSURE
MINIMUM EXPERIMENTAL PRESSURE
EXPERIMENTAL DATA
LINEAR REGRESSION CURVE

Table 5.1. Results of tests to determine the compliance of latex tube #1

Run #	Compliance, C, m^4/N	
	Direct measurements	Dynamic tests
1	1.56×10^{-10}	1.45×10^{-10}
2	1.59×10^{-10}	1.66×10^{-10}
3	$1.65 \times 1-^{-10}$	1.71×10^{-10}
4	1.59×10^{-10}	1.62×10^{-10}
5	1.61×10^{-10}	1.54×10^{-10}
Mean±S.D.	$(1.60 \pm 0.03) \times 10^{-10}$	$(1.60 \pm 0.08) \times 10^{-10}$

Table 5.2. Results of tests to determine the compliance of latex tube #2

Run #	Compliance, C, m^4/N	
	Direct measurements	Dynamic tests
1	2.48×10^{-10}	2.52×10^{-10}
2	2.46×10^{-10}	2.68×10^{-10}
3	2.47×10^{-10}	2.56×10^{-10}
4	2.34×10^{-10}	2.41×10^{-10}
5	2.40×10^{-10}	2.50×10^{-10}
Mean±S.D.	$(2.43 \pm 0.05) \times 10^{-10}$	$(2.53 \pm 0.09) \times 10^{-10}$

Fig. 5.3. Comparison of pressure waveforms measured by UET and pressure transducer

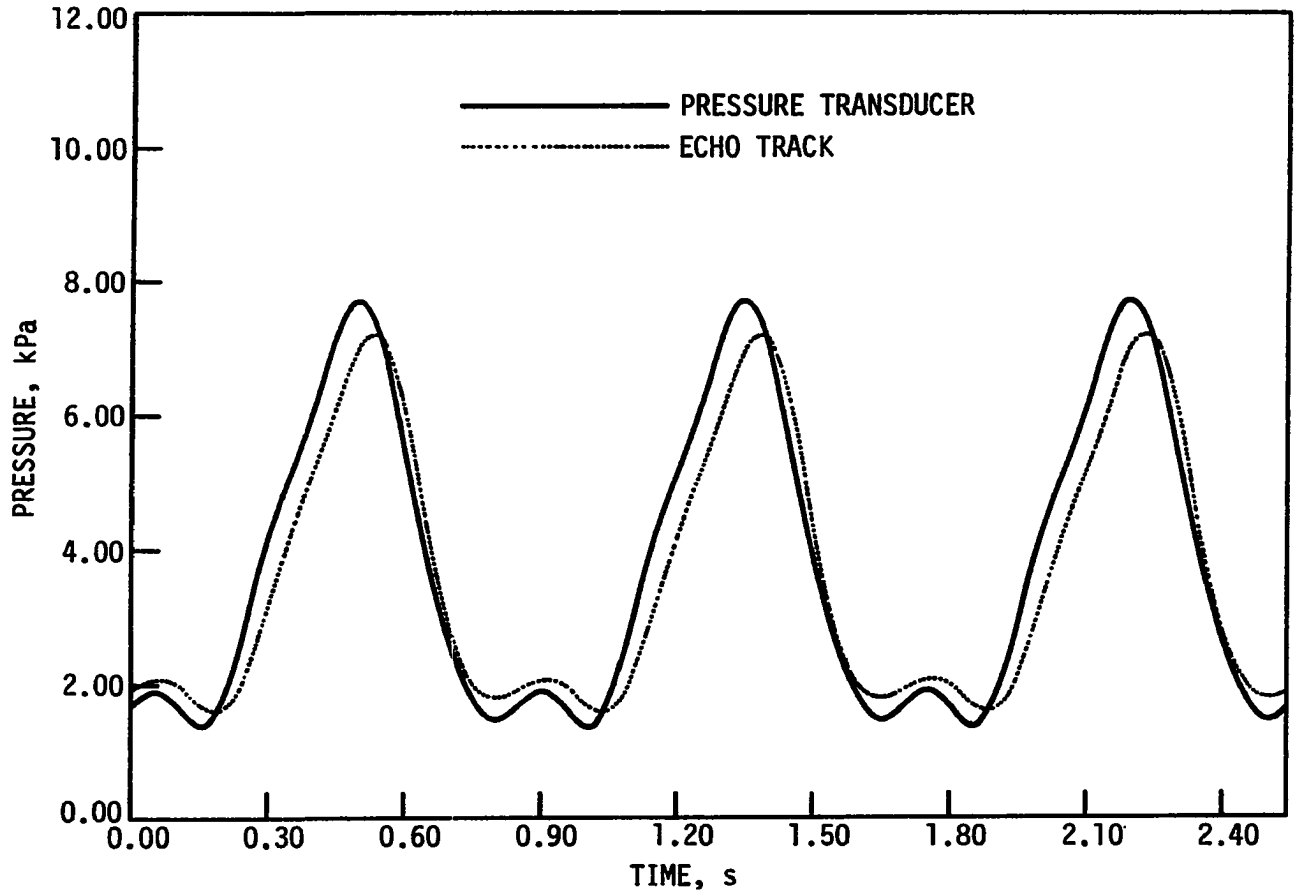
PRESSURE TRANSDUCER
ECHO TRACK
PRESSURE, kPa
12.00
10.00
8.00
6.00
4.00
2.00
0.00
0.00
0.30
0.60
0.90
1.20
1.50
1.80
2.10
2.40
TIME, s

study were essentially the same as the ones used by Rooz (1980), no additional effort was made to validate the model. However, the parameter estimation scheme was tested in model-to-model tests to see if it would yield reasonable estimates for the parameters of interest. The validation of the scheme was carried out by initially defining the values of all the parameters in the model. The model was then solved and the pressure and flow waveforms predicted by the model were stored and used for subsequent model fitting. In the model-to-model tests, the proximal flow and a lumped linear distal resistance were used as boundary conditions and the proximal pressure waveform generated by the model was used for model fitting. This method of testing eliminates modeling and measurement inaccuracies and any discrepancy between the estimated value of the parameters and those used to produce the model input can be attributed to the inaccuracies in the estimation algorithm.

A summary of the model-to-model test results is given in Table 5.3. In these tests, it was assumed that stenoses of different severity were placed midway along the length of the tube and the model was solved to produce a proximal pressure waveform for use as an estimator. The starting values of the parameters of interest (the location and the severity of the stenoses) corresponded to a stenosis with a 99.0% area reduction located 3/4 of the way along the length of the tube from the proximal measurement site. All other parameters were assumed to be known. The scheme was used to produce the best estimates for these parameters based on the convergence criteria outlined in Chapter 4. In all cases, the model-to-model tests yielded good results in that the estimated values of the

Table 5.3. Summary of model-to-model parameter estimation results for an obstructed tube

Run #	Mean Re[b]	Peak Re[c]	α[d]	Experimental value D, mm	Experimental value L, mm	Estimated value D, mm	Estimated value L, mm	Error (%)[a] D	Error (%)[a] L
1	282	541	8.9	1.51 (94.3%)[e]	160.00	1.48 (94.6%)	159.00	1.98	0.62
2	309	539	9.2	2.47 (86.0%)	153.00	2.37 (86.0%)	152.00	0.00	0.65
3	584	805	9.1	3.18 (74.8%)	160.00	3.18 (74.8%)	160.00	0.00	0.00
4	415	926	8.9	4.31 (53.8%)	160.00	3.56 (68.4%)	160.00	17.00	0.00

[a] Error % = ((experimental value-estimated value)/experimental value) x100.

[b] Mean Re = $\frac{V_{mean} D_{tube} \rho}{\mu}$.

[c] Peak Re = $\frac{V_{peak} D_{tube} \rho}{\mu}$.

[d] $d_\alpha = \frac{D_{tube}}{2} \sqrt{\frac{\omega}{\nu}}$.

[e] Figures in parentheses denote percent stenoses. Percent stenosis = $(1 - \frac{\text{minimum area of stenosis}}{\text{cross-sectional area of tube}}) \times 100$.

parameters were very close to the corresponding values used to generate the model input as shown in Table 5.3. When the estimation scheme was used to estimate the stenosis parameters for stenoses ranging in severity from 94.3% to 74.8%, the maximum difference between the model and estimated parameter values represented an error of 1.98% based on model parameter value for the diameter of a 94.3% stenosis. It can be seen

from Table 5.3 that an attempt to estimate the stenosis characteristics for a 53.8% stenosis produced an error of 17.00% between the model and estimated diameters. This relatively large error could have been caused by the fact that such mild stenoses do not produce significant changes in the pressure and flow waveforms which were used as input to the estimation scheme. It was, therefore, decided that model-to-experiment tests on the hydraulic model would be conducted to predict the stenosis characteristics of stenoses representing a reduction in cross-sectional area of 74.8% or more.

Experiments with Unobstructed Tubes

Invasive and noninvasive pressure and flow measurements were obtained from tests on an unobstructed tube of known length and inner diameter. The invasive data were used as input into the estimation scheme to estimate the compliance of the tube and the value of the distal resistance, Z. In these tests, the proximal flow and the distal resistance were used as boundary conditions to solve the model, and the measured proximal pressure was used for model fitting. The estimated value of the compliance was compared with that predicted by the UET. The noninvasively obtained data were then used as input into the estimation scheme to estimate the distal resistance using the same boundary conditions and estimator as above. The estimated value of the resistance was compared with the measured experimental value and that estimated when invasive data were used as input into the estimation scheme. The results of these tests are summarized in Table 5.4. It can be seen that the estimated value of the compliance corresponds well with that predicted by the UET. Also, the estimated values

Table 5.4. Summary of model-to-experiment parameter estimation results

Run #	Mean Re[b]	Peak Re[c]	α[d]	Data input	Experimental value C, m^4/N	Experimental value Z, N-s/m^5	Estimated value C, m^4/N	Estimated value Z, N-s/m^5	Error (%)[a] C	Error (%)[a] Z
1	389	803	9.1	invasive	0.92×10^{-10}	2.31×10^{9}	1.02×10^{-10}	2.13×10^{9}	-10.87	7.79
2	442	881	9.1	noninvasive	0.92×10^{-10}	2.31×10^{9}	*	2.24×10^{9}	*	3.03

[a] Error % = ((experimental value-estimated value)/experimental value)x100.

[b] Mean Re = $\frac{V_{mean} D_{tube} \rho}{\mu}$.

[c] Peak Re = $\frac{V_{peak} D_{tube} \rho}{\mu}$.

[d] $d_\alpha = \frac{D_{tube}}{2}\sqrt{\frac{\omega}{\nu}}$.

of the distal resistance obtained when invasive or noninvasive data were used as input show close correlation with each other, and with the experimentally measured value. A plot of the proximal flow waveform obtained by using the USF and that obtained by using the EMF is shown in Fig. 5.4. It can be seen that the waveforms match reasonably well. A similar match between the flow waveforms measured by the USF and the EMF was seen in other dynamic tests.

Experiments with Obstructed Tubes

The results of the tests with obstructed tubes are presented in Tables 5.5 and 5.6. Table 5.5 represents the results when invasive (direct) measurements of the system variables were used as input into the estimation scheme and Table 5.6 summarizes the results when noninvasive measurements of the system variables were used as input. In most cases, there is good agreement between the estimated values of the parameters and the corresponding experimentally measured values whether invasive or noninvasive measurements were used as inputs into the estimation scheme. Figure 5.5 shows the experimentally measured invasive proximal pressure waveform used for model fitting, and that generated by the model with the best estimates for the stenosis parameters for a 86.0% stenosis placed centrally in the tube. From Table 5.5, it can be seen that the difference between the estimated and the experimental values of the diameter and the location of the stenosis in this run are 0.42% and 2.42%, respectively. Thus, this figure represents best match between the measured and model

Fig. 5.4. Comparison of flow waveforms measured by USF and EMF

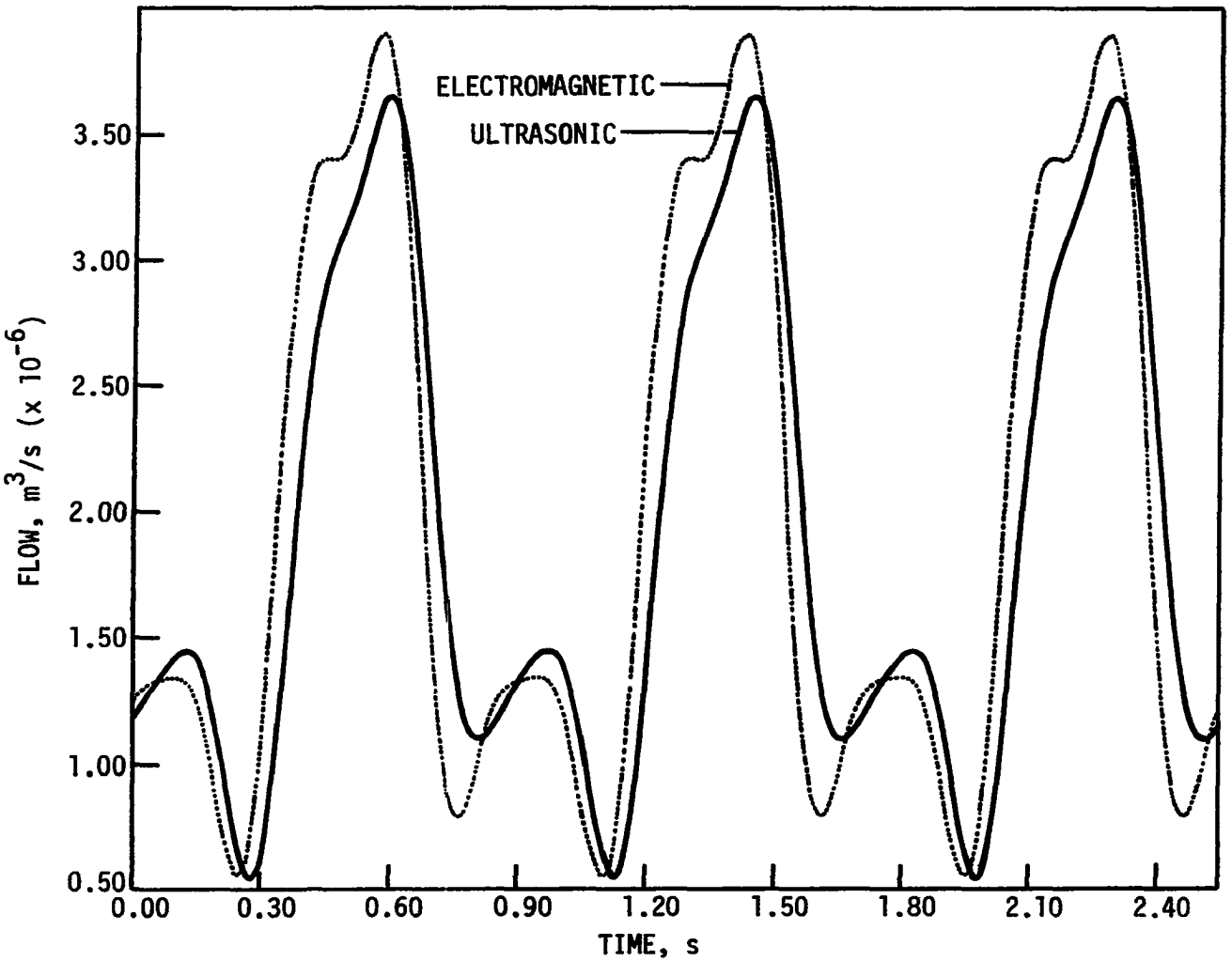
ELECTROMAGNETIC
ULTRASONIC
FLOW, m³/s (x 10⁻⁶)
3.50
3.00
2.50
2.00
1.50
1.00
0.50
0.00
0.30
0.60
0.90
1.20
1.50
1.80
2.10
2.40
TIME, s

Table 5.5. Summary of model-to-experiment parameter estimation results using invasive input data

Run #	Mean Re[b]	Peak Re[c]	α[d]	Experimental value D, mm	Experimental value L, mm	Estimated value D, mm	Estimated value L, mm	Error (%)[a] D	Error (%)[a] L
1	367	760	9.0	1.51 (94.3%)[e]	192.00	1.71 (92.7%)	220.00	-13.25	-14.58
2	341	696	9.2	2.37 (86.0%)	192.00	2.36 (86.1%)	196.64	0.42	2.42
3	212	440	9.0	3.18 (74.8%)	192.00	2.90 (72.1%)	212.00	8.81	-10.42

[a] Error % = ((experimental value-estimated value)/experimental value) x100.

[b] Mean Re = $\frac{V_{mean} D_{tube} \rho}{\mu}$.

[c] Mean Re = $\frac{V_{peak} D_{tube} \rho}{\mu}$.

[d] $d_\alpha = \frac{D_{tube}}{2} \sqrt{\frac{\omega}{\nu}}$.

[e] Figures in parentheses denote percent stenoses. Percent stenosis = $(1 - \frac{\text{minimum area of stenosis}}{\text{cross-sectional area of tube}})$x100.

generated waveforms. The match between the waveforms in the other tests though reasonable was not as close.

In all test cases, the proximal flow and distal resistance, Z, were used as boundary conditions and the measured proximal pressure was used for model fitting. An appropriate value of Z was obtained by dividing the mean proximal pressure by the mean proximal flow. It was realized that the choice of such an approximate value for Z would lead to errors in the estimates. However, the aforementioned choice of boundary conditions and

Table 5.6. Summary of model-to-experiment parameter estimation results using noninvasive input data

Run #	Mean Re[b]	Peak Re[c]	α[d]	Experimental value D, mm	Experimental value L, mm	Estimated value D, mm	Estimated value L, mm	Error (%)[a] D	Error (%)[a] L
1	282	541	8.9	1.51 (94.3%)[e]	160.00	1.44 (94.8%)	192.00	4.64	20.00
2	309	539	9.2	2.37 (86.0%)	153.00	2.50 (84.5%)	151.93	-5.48	6.34
3	584	805	9.1	3.18 (74.8%)	160.00	3.35 (72.1%)	173.14	-5.17	6.34

[a]Error % = ((experimental value-estimated value)/experimental value) x100.

[b]Mean Re = $\frac{V_{mean} D_{tube} \rho}{\mu}$.

[c]Peak Re = $\frac{V_{peak} D_{tube} \rho}{\mu}$.

[d]$d_\alpha = \frac{D_{tube}}{2} \sqrt{\frac{\omega}{\nu}}$.

[e]Figures in parentheses denote percent stenoses. Percent stenosis = $(1 - \frac{\text{minimum area of stenosis}}{\text{cross-sectional area of tube}})$x100.

estimator requires that only the proximal flow and pressure be measured for input to the model. This represents the minimum number (2) of measurements needed to estimate the parameters. It was hoped that minimizing the number of measurements would reduce the errors in estimates due to measurement errors, which could be considerable in a physiologic situation. It was also felt that such a choice of boundary conditions and estimator would make the scheme simpler to implement and make it useful as a possible noninvasive diagnostic tool in a clinical setting. The results

Fig. 5.5. Comparison of invasively measured proximal pressure and model generated proximal pressure after convergence for a 85.0% stenosis located centrally in the tube

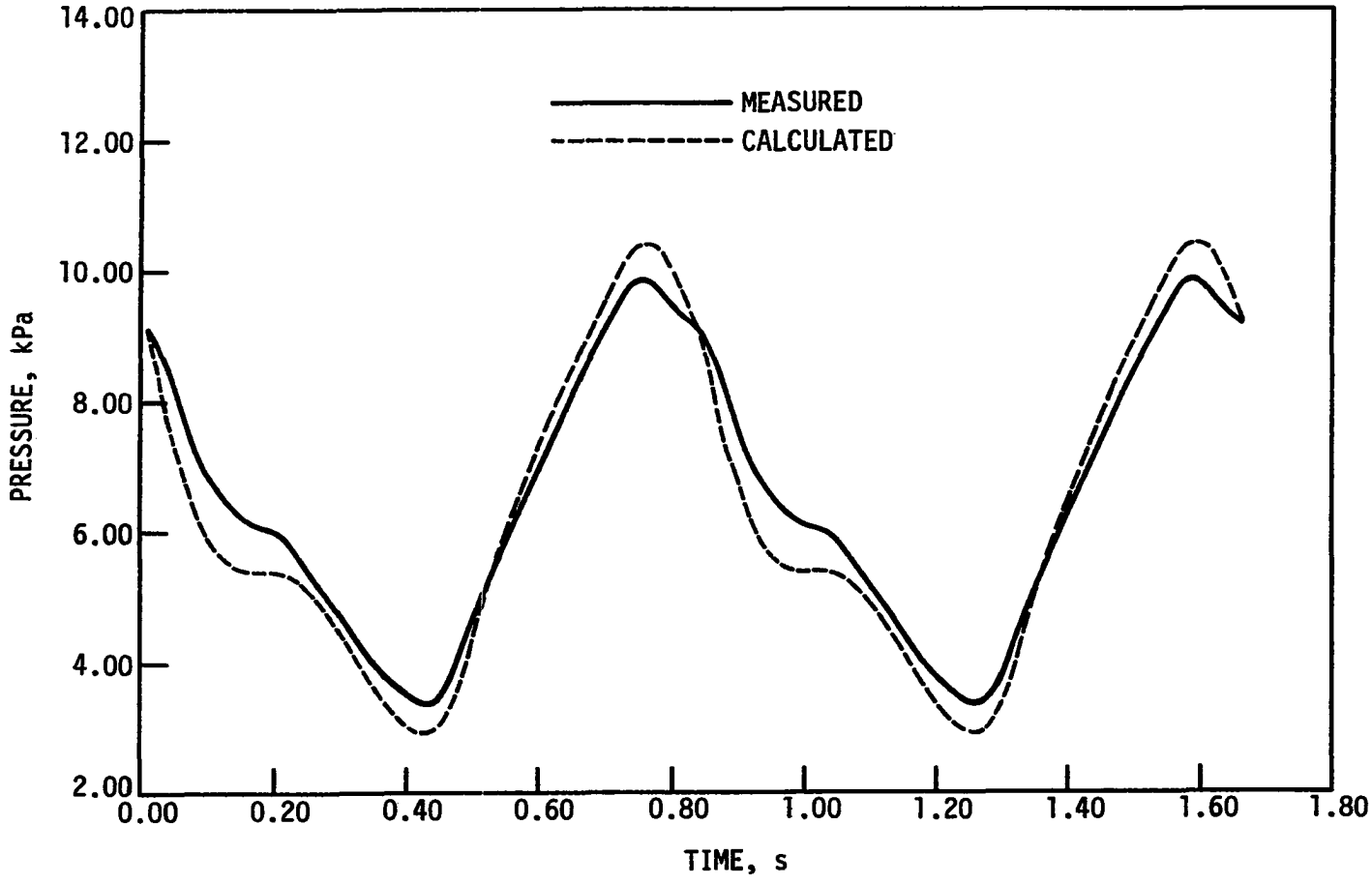
14.00
12.00
10.00
8.00
6.00
4.00
2.00
PRESSURE, kPa
MEASURED
CALCULATED
0.00
0.20
0.40
0.60
0.80
1.00
1.20
1.40
1.60
1.80
TIME, s

of the model-to-experiment tests summarized in Tables 5.5 and 5.6 suggest that this choice the boundary conditions and estimator made in this study were appropriate.

The error in the estimates due to the use of an approximate value for Z would be higher in the case of a 94.30% stenosis where the ratio of mean proximal pressure to the mean distal pressure would be higher than that in the case of a 84.3% or a 74.3% stenosis. Thus, the value of Z chosen as above in the case of a severe stenosis would be higher than the actual experimental value. This could lead to errors in estimates for the severity and the location of the stenosis. Tests were run with invasive and noninvasive data to try and estimate the value of Z in addition to the stenosis parameters for a 94.3% stenosis. These tests yielded fairly accurate estimates for the diameter but the estimates for the location were considerably different from the experimentally measured values. This could be due to the fact that the solution is far more sensitive to changes in the diameter and the distal resistance than it is to the changes in the location of the stenosis. Also, it is felt that some of the errors in the estimates could have been caused by the use of too few measured data as input to the estimation scheme. Figure 5.6 shows the noninvasively measured proximal pressure waveform for a 94.3% stenosis and the one generated by the model with all the model parameters set at their experimentally measured values. The mismatch between the waveforms is indicative of the measurement errors. A similar comparison of the distal waveform generated by the model and that measured noninvasively is shown in Fig. 5.7.

Fig. 5.6. Comparison of noninvasively measured proximal pressure with model generated proximal pressure for a 94.6% stenosis located centrally in the tube; model parameters set at experimental values

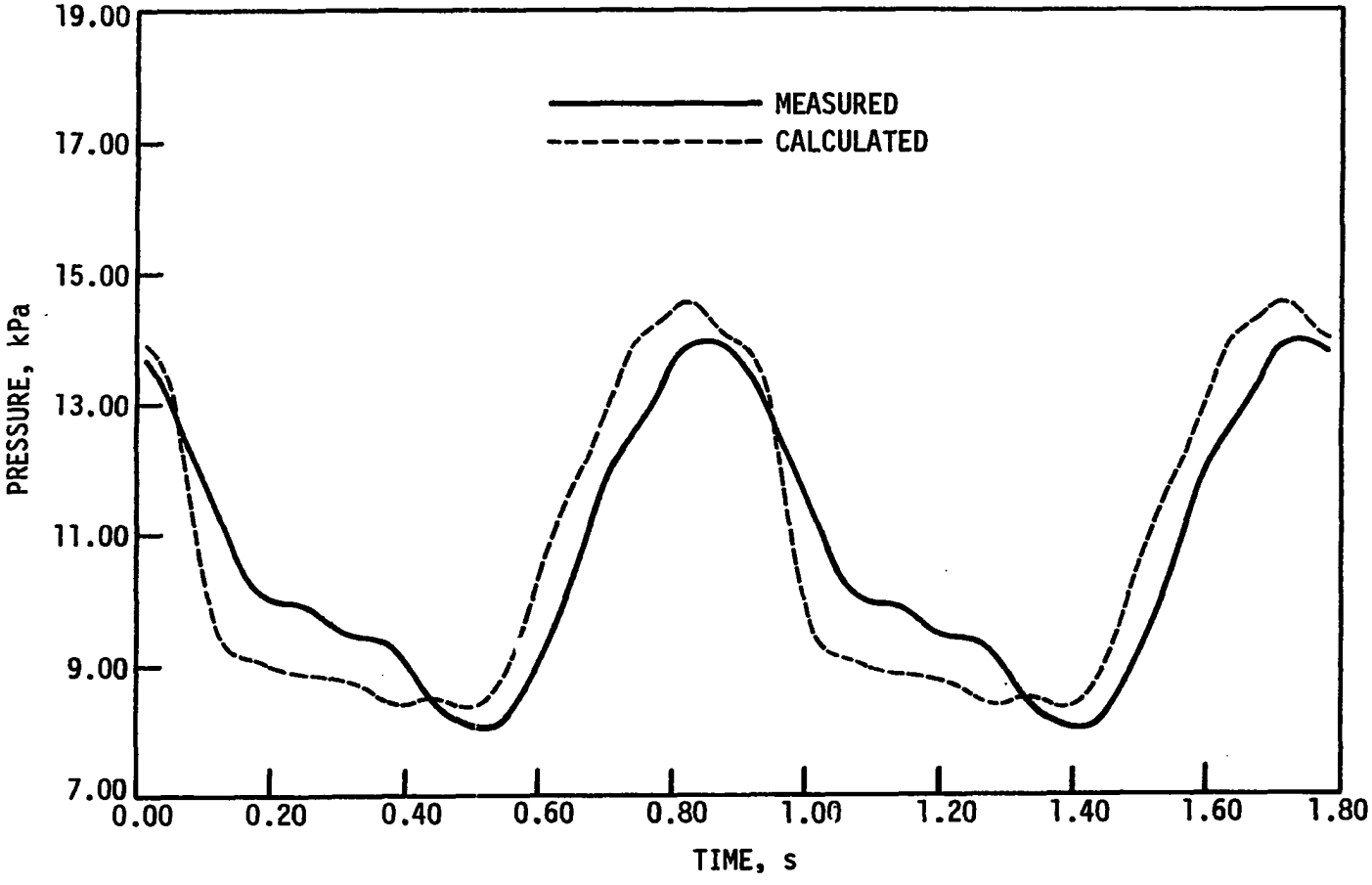
MEASURED
CALCULATED
PRESSURE, kPa
19.00
17.00
15.00
13.00
11.00
9.00
7.00
0.00
0.20
0.40
0.60
0.80
1.00
1.20
1.40
1.60
1.80
TIME, s

Fig. 5.7. Comparison of noninvasively measured distal pressure with model generated distal pressure for a 94.6% stenosis located centrally in the tube; model parameters set at experimental values

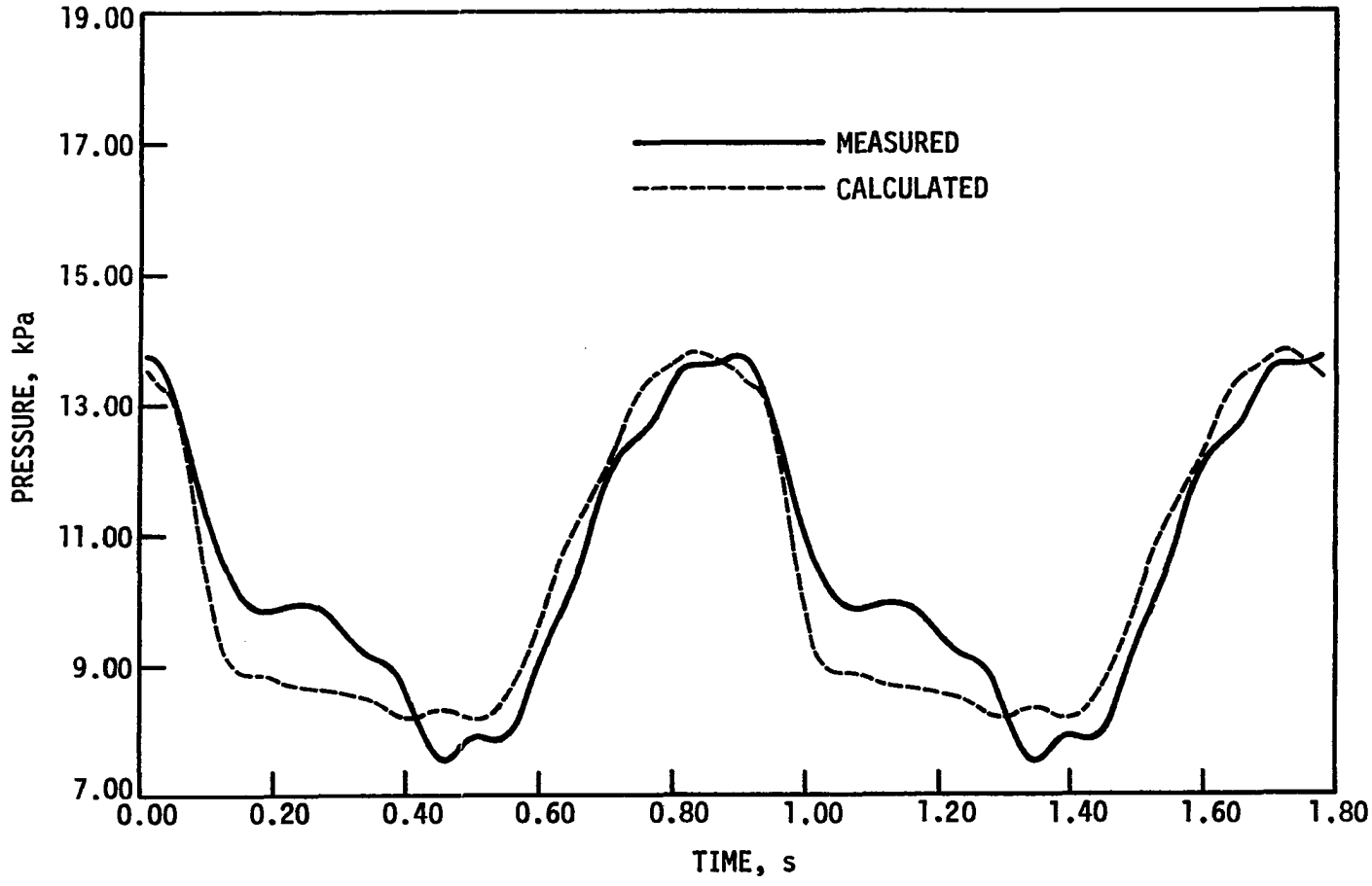
19.00
17.00
15.00
13.00
11.00
9.00
7.00
PRESSURE, kPa
MEASURED
CALCULATED
0.00
0.20
0.40
0.60
0.80
1.00
1.20
1.40
1.60
1.80
TIME, s

At this point, it should be mentioned that an effort to estimate the stenosis parameters by using the proximal flow and the distal pressure as boundary conditions with the measured proximal pressure as an estimator yielded very poor estimates when the parameters were estimated individually or in combination. The reason for this is not known but could be attributed to the sensitivity of the numerical scheme to the pressure measurements so that any small errors in the measured pressure used as a distal boundary condition would yield poor estimates. This seems to be supported by the results of Young et al. (1980) who suggested that the proximal flow and distal resistance boundary conditions yielded the best estimates for the model parameters.

Animal Experiments

To further assess the feasibility of using parameter estimation for physiologic studies, invasive pressure and flow measurements obtained from the femoral arteries of mongrel dogs were used as input to the estimation scheme to estimate the stenosis parameters. The very short arterial test section and the stiffening effects of the plug used to simulate a stenosis precluded efforts to estimate the value of the compliance of the vessel. Thus, in all animal tests, the value of the compliance was calculated from the equation

$$C = A/(\rho c^2) \tag{5.1}$$

where

C = compliance of the vessel

A = nominal cross-sectional area of the vessel

ρ = density of the blood

c = velocity of pressure pulse propagation in the artery taken to 10.00 m/s

This equation is similar to the one that governs the speed of propagation of waves in a stretch string and can be derived by considering the balance between the inertia of the mass of blood, characterized by the blood density, and the restoring forces of the elastic walls. The value of 10.00 m/s for the velocity of pressure pulse propagation in the artery was obtained from Caro et al. (1978). In the animal tests, a very coarse grid was used, i.e., there were only two nodes each proximal and distal to the stenosis. An attempt to use a larger number of nodes led to poor parameter estimates due to instabilities in the numerical solution scheme unless it was accompanied by a grid size refinement in the time direction also. Grid size refinement in both time and spatial direction would have led to increased computational cost and was not attempted. It is pertinent to mention that when three elements were used to represent the arterial segment, the ratio of length step to the time step was of the same order of magnitude as that used in the hydraulic model tests. It was expected that use of a coarse grid, and the arbitrarily assigned value of the compliance, would probably lead to rather poor estimates for the parameters.

The results of the animal experiments are summarized in Table 5.7. Surprisingly, it was possible to obtain reasonably good estimates for the severity of the stenoses, although the quality of the match between the measured proximal pressure waveform and that predicted by the model was not as good as the one obtained in hydraulic model tests. This mismatch

Table 5.7. Summary of model-to-experiment parameter estimation results

Run #	Mean Re[b]	Peak Re[c]	α[d]	Experimental value D, mm	Estimated value D, mm	Error (%)[a] D
1	153	169	3.9	1.42 (90.0%)[e]	1.59 (87.5%)	11.90
2	303	402	3.8	1.26 (90.0%)	1.39 (87.9%)	-10.30
3	269	362	4.7	2.75 (75.0%)	1.96 (87.4%)	28.70
4	200	387	3.7	2.00 (75.0%)	2.04 (73.9%)	-2.00
5	269	537	3.7	2.53 (60.0%)	2.64 (56.4%)	4.30

[a] Error % = ((experimental value-estimated value)/experimental value) x100.

[b] Mean Re = $\frac{V_{mean} D_{vessel} \rho}{\mu}$.

[c] Peak Re = $\frac{V_{peak} D_{vessel} \rho}{\mu}$.

[d] $d_{\alpha} = \frac{D_{vessel}}{2} \sqrt{\frac{\omega}{\nu}}$.

[e] Figures in parentheses denote percent stenoses. Percent stenosis = $(1 - \frac{\text{minimum area of stenosis}}{\text{cross-sectional area of tube}})$x100.

could have been caused by the use of a coarse grid in the solution scheme and the use of an approximate value for the compliance of the vessel. A perusal of Tables 5.5, 5.6 and 5.7 shows that the difference between the estimated and experimentally measured values in the animal experiments is generally of the same order of magnitude as those for the hydraulic model experiments.

CHAPTER 6. DISCUSSION AND SUMMARY

The UET was found to yield good estimates for the compliance of the tubes used in the hydraulic model. Also, the diameter-change waveform measured by the UET could be transformed to yield the pressure pulse waveform. In addition, the flow waveforms measured by the USF agreed reasonably well with those measured by the EMF.

The feasibility of using noninvasively measured values of the system variables to obtain reasonable estimates for model parameters in an obstructed and unobstructed tube has been established in this study. The estimates for the model parameters based on noninvasive measurements compare well with the experimentally measured values, and also with the estimates based on invasive measurements. Since the model-to-model tests yielded very accurate estimates, it is felt that any inaccuracies in the model-to-experiment estimates can be attributed to measurement errors.

Limited in-vivo experiments on mongrel dogs also suggest the feasibility of obtaining reliable estimates for the stenosis parameters in a physiological system. These estimates were based on invasive measurements.

The aim of this study was to systematically explore the possibility of measuring the system variables accurately, and to use these values as input into the estimation scheme to obtain reasonable estimates for the system parameters. It is believed that this aim has been fulfilled.

However, to apply the parameter estimation scheme in a more generalized form to physiological systems, it is felt that further research is

needed in the following areas:

1. A more general model of the arterial tree which incorporates branches and allows for the tapering of the vessel and the variation in the compliance along the length of the vessel is needed. The model should also incorporate a nonlinear area-pressure relationship for the vessel wall. Porenta (1982) has formulated such a model and it can be used in conjunction with the parameter estimation scheme to carry out further research in estimating parameters in a physiological system. The work currently under way in the ISU Biomedical Fluid Mechanics Laboratory to obtain castings of the femoral arteries of dogs may yield good values for the vessel taper function and realistic values for the sizes of the main branches from the artery. These data could be incorporated into the model proposed by Porenta (1982) to represent the physiological system more accurately.
2. It is felt that some form of analysis of the Fourier coefficients of the flow and pressure waveforms used as input data for the estimation scheme is necessary. Such an analysis could be used to establish the relative importance of the various terms in the Fourier series representation of the input waveforms. It is felt that the use of filtered input and output data in the parameter estimation scheme may lead to better and more consistent estimates. A study conducted by Oakland and Herd (1982) could form the basis for the analysis of the input data.
3. In spite of the fairly good results achieved in this study, it is felt that the parameter estimation technique is still an art in its present

state. Further research is needed to generate regions of confidence for the final estimates.

In conclusion, the results of this study indicate that the parameter estimation technique based on noninvasive measurements of the system variables can be a useful tool to diagnose arterial diseases. It is felt that this study could form the basis for further research efforts to generalize the arterial model, and to obtain reasonably accurate noninvasively obtained input data for the estimation scheme.

REFERENCES

Anliker, M., R. L. Rockwell and E. Ogden. 1971a. Nonlinear analysis of flow pulses and shock waves in arteries: I. Derivation and properties of mathematical model. Zeitschrift für Angewandte Mathematik und Physik 22:217-246.

Anliker, M., R. L. Rockwell and E. Ogden. 1971b. Nonlinear analysis of flow pulses and shock waves in arteries: II. Parametric study related to clinical problems. Zeitschrift für Angewandte Mathematik und Physik 22:563-581.

Anliker, M., J. C. Stettler, P. Niederer and R. Holenstein. 1978. Prediction of shape changes of propagation flow and pressure pulses in human arteries. Pages 15-34 in R. D. Bauer and R. Busse, eds. The arterial system: Dynamics, control theory and regulation. Springer-Verlag, Berlin.

Beck, J. V. and K. J. Arnold. 1977. Parameter estimation in engineering and science. John Wiley and Sons, New York.

Bekey, G. A. and S. M. Yamashiro. 1976. Parameter estimation in mathematical model of biological systems. Advances in Biomedical Engineering 6:1-43.

Beneken, J. E. W. 1972. Some computer models in cardiovascular research. Pages 173-223 in D. H. Bergel, ed. Cardiovascular fluid dynamics. Volume I. Academic Press, London.

Bernstein, E. F., A. E. Murphy, M. A. Shea and L. B. Housman. 1970. Experimental and clinical experience with transcutaneous Doppler ultrasonic flowmeters. Archives of Surgery 101:21-25.

Bourne, P. R. and R. I. Kitney. 1978. Matching techniques for clinical models of the circulation. Medical and Biological Engineering and Computing 16:689-696.

Caro, C. G., T. J. Pedley, R. C. Schroter and W. A. Seed. 1978. The mechanics of the circulation. Oxford University Press, New York.

Chang, P. R., G. L. Matson, J. E. Kendrick and V. C. Rideout. 1974. Parameter estimation in the canine cardiovascular system. IEEE Transactions on Automatic Control AC-19:927-931.

Clark, J. W., Jr., R. Y. S. Ling, R. Srinivasan, J. S. Cole and R. C. Pruitt. 1980. A two-stage identification scheme for the determination of the parameters of a model of the left heart and systemic circulation. IEEE Transactions on Biomedical Engineering BME-27: 20-29.

Gray, T. A. 1981. Indirect estimation of parameters in a flexible tube, pulsatile flow system. Ph.D. Thesis. Iowa State University, Ames.

Hankner, D. O. 1978. Measurement of pulsatile flow characteristics with ultrasonic and electromagnetic flowmeters. M.S. Thesis. Iowa State University, Ames.

Hokanson, D. E., D. J. Mozersky, D. S. Sumner and D. E. Strandness, Jr. 1972. A phase-locked echo tracking system for recording arterial diameter changes in vivo. Journal of Applied Physiology 5:728-733.

Holenstein, R. and P. Niederer. 1980. Propagation and damping of flow and pressure pulses in the human arterial tree. Proceedings of the International Conference on Finite Elements in Biomechanics 1:315-328.

Lunt, M. J. 1975. Accuracy and limitations of the ultrasonic Doppler blood velocimeter and zero crossing detector. Ultrasound in Medicine 2:1-10.

Moss, S. and D. Bennett. 1979. A combined transcutaneous pulse-echo and Doppler ultrasonic technique for the measurement of brachial artery peak velocities. Journal of Biomedical Engineering 1:5-11.

Mozersky, D. J., D. S. Sumner, D. E. Hokanson and D. E. Strandness, Jr. 1972. Transcutaneous measurement of the elastic properties of the human femoral artery. Circulation 46:948-955.

Newman, D. L., N. Westerhof and P. Sipkema. 1979. Modeling of aortic stenosis. Journal of Biomechanics 12:229-235.

Noordergraaf, A. 1978. Circulatory system dynamics. Academic Press, New York.

Noordergraaf, A., P. D. Verdouw, A. G. von Brummelen and F. W. Wiegel. 1964. Analog of the arterial bed. Pages 373-388 in E. O. Attinger, ed. Pulsatile blood flow. McGraw-Hill, New York.

Oakland, S. and H. Herd. 1982. Data reduction, curve fitting and separation of signal from noise. IBM Report. IBM, Rochester, MN.

Olsen, J. H. and A. H. Shapiro. 1967. Large-amplitude unsteady flow in liquid-filled elastic tubes. Journal of Fluid Mechanics 29:513-538.

Porenta, G. P. 1982. A computer based feasibility analysis of assessing arterial flow using pulsatility indices. M.S. Thesis. Iowa State University, Ames.

Raines, J. K., M. Y. Jaffrin and S. Rao. 1973. A noninvasive pressure-pulse recorder: Development and rationale. Medical Instrumentation 4:245-250.

Raines, J. K., M. Y. Jaffrin and A. H. Shapiro. 1974. A computer simulation of arterial dynamics in the human leg. Journal of Biomechanics 7:77-91.

Reagen, J. R., C. W. Miller and D. E. Strandness, Jr. 1971. Transcutaneous measurement of femoral artery flow. Journal of Surgical Research 11:477-482.

Rideout, V. C. and J. E. W. Beneken. 1975. Parameter estimation applied to physiological systems. Proceedings of the International Association for Analog Computation 17:23-36.

Rooz, E. 1980. A finite element simulation of pulsatile flow in flexible tubes. Ph.D. Thesis. Iowa State University, Ames.

Rumberger, J. A. and R. M. Nerem. 1977. A method-of-characteristics calculation of coronary blood flow. Journal of Fluid Mechanics 32: 429-448.

Satomura, S. 1959. A study of flow patterns in peripheral arteries by ultrasonics. Journal of the Acoustical Society of Japan 15:151-158.

Schaaf, B. W. and P. H. Abbrecht. 1972. Digital computer simulation of human arterial pulse wave transmission: A nonlinear model. Journal of Biomechanics 5:345-364.

Seeley, B. D. and D. F. Young. 1976. Effect of geometry on pressure losses across models of arterial stenoses. Journal of Biomechanics 9:439-448.

Shoor, P. M., A. Fronek and E. F. Bernstein. 1979. Quantitative transcutaneous arterial velocity measurements with Doppler flowmeters. Archives of Surgery 114:922-928.

Sims, J. B. 1972. Estimation of arterial system parameters from dynamic records. Computers and Biomedical Research 5:131-147.

Snyder, M. F. and V. C. Rideout. 1968. Computer modeling of the human systemic arterial tree. Journal of Biomechanics 1:341-353.

Stettler, J. C., P. Niederer and M. Anliker. 1981. Theoretical analysis of arterial hemodynamics including the influence of bifurcations. I. Mathematical model and prediction of normal pulse patterns. Annals of Biomedical Engineering 9:145-164.

Streeter, V. L., W. F. Keitzer and D. F. Bohr. 1963. Pulsatile pressure and flow through distensible vessels. Circulation Research 13:3-20.

Taylor, M. G. 1965. Wave travel in a non-uniform transmission line, in relation to pulse in arteries. Physics in Medicine and Biology 10: 539-550.

Vander Werff, T. J. 1974. Significant parameters in arterial pressure and velocity development. Journal of Biomechanics 7:437-447.

Welkowitz, W. 1977. Engineering hemodynamics: Application to cardiac assist devices. D. C. Heath and Company, Lexington, Massachusetts.

Wemple, R. R. and L. F. Mockros. 1972. Pressure and flow in systemic arterial system. Journal of Biomechanics 5:629-641.

Wesseling, K. H., B. deWitt and J. E. W. Beneken. 1973. Arterial hemodynamic parameters derived from noninvasively recorded pulsewaves using parameter estimation. Medical and Biological Engineering 11: 724-731.

Westerhof, N. and A. Noordergraaf. 1970. Arterial viscoelasticity: A generalized model: Effect on input impedance and wave travel in the systemic tree. Journal of Biomechanics 3:357-379.

Westerhof, N., F. Bosman, C. J. deVries and A. Noordergraaf. 1969. Analog studies of the human systemic arterial tree. Journal of Biomechanics 2:121-143.

Young, D. F. 1979. Fluid mechanics of arterial stenoses. Journal of Biomedical Engineering 101:157-175.

Young, D. F. and F. Y. Tsai. 1973a. Flow characteristics in models of arterial stenosis: I. Steady flow. Journal of Biomechanics 6:395-410.

Young, D. F. and F. Y. Tsai. 1973b. Flow characteristics in models of arterial stenosis: II. Unsteady flow. Journal of Biomechanics 6: 547-559.

Young, D. F., N. R. Cholvin and A. C. Roth. 1975. Pressure drop across artificially induced stenoses in the femoral arteries of dogs. Circulation Research 36:735-743.

Young, D. F., T. R. Rogge, T. A. Gray and E. Rooz. 1980. Indirect evaluation of system parameters for pulsatile flow in flexible tubes. Journal of Biomechanics 5:339-347.

ACKNOWLEDGMENTS

I would like to thank Professor Donald F. Young for the technical and financial assistance I received during the course of this study and also for the courtesy and understanding he showed when I encountered problems during the course of this study. My thanks also to Professor Thomas R. Rogge for cheerfully disregarding the many mistakes I made and for steering me on to the right track. I am grateful to Pamela K. McAllister who did the surgery for the animal experiments and to Barbara N. Steele who typed parts of this thesis. Additional thanks are due to Professors David L. Carlson, Bruce R. Munson and Richard H. Pletcher for serving on my committee and for agreeing to examine me at a very short notice. Rodney E. Lee introduced me to the complexities of the PDP-11 computer and I would like to thank him for all the fun I had with this machine. Finally, I would like to thank my wife, Carolyn, who encouraged me, and the faculty, staff and students of the Biomedical Engineering Program who made me feel at home and my stay at ISU an enjoyable one.

APPENDIX

A summary of the data analysis program used to calculate the compliance of the tube from dynamic tests and to transform the vessel diameter-change waveform into the pressure pulse is given in this section.

In each dynamic test, the following data were recorded:

$P(t)$ = digitized value corresponding to the instantaneous pressure

$E(t)$ = digitized value corresponding to the diameter of the tube

These data were analyzed to obtain the maximum and minimum values of $P(t)$ and $E(t)$. Let

P_{max} = digitized value corresponding to the maximum pressure in a cycle

P_{min} = digitized value corresponding to the minimum pressure in a cycle

E_{max} = digitized value corresponding to the maximum diameter of the tube in a cycle

E_{min} = digitized value corresponding to the minimum diameter of the tube in a cycle

The calibration tests for the pressure transducer yielded the slope of the calibration curve, S (pressure/digit), and the intercept, I (digits). The calibration test for the UET yielded a calibration constant, B (mm/digit).

Now, the compliance is defined as the change in cross-sectional area of the tube per unit change in the pressure in the tube. Or, if A and a are the maximum and minimum cross-sectional areas of the tube corresponding to the pressures P and p, then the compliance C can be calculated by using Eq. (A.1).

$$C = (A - a)/(P - p) \qquad (A.1)$$

$$C = (\pi(D - d)^2)/(4(P - p))$$

$$= (\pi(D - d)(D + d))/(4(P - p))$$

where

D = maximum diameter of the tube in a cycle

d = minimum diameter of the tube in a cycle

If it is assumed that the maximum change in the diameter over a cycle is small compared to some mean diameter, D_0, i.e.,

$$(D - d) << D_0$$

where D_0 is the mean diameter of the tube. Then, the compliance can be calculated from Eq. (A.2)

$$C = (2\pi D_0(D - d))/(4(P - p)) \qquad (A.2)$$

Equation (A.2) can be written in terms of the recorded experimental data as

$$C = (\pi D_0 B(E_{max} - E_{min}))/(2S(P_{max} - P_{min}))$$

In the above equation, the value of D_0, the mean diameter can be obtained either by direct measurement or by using the UET.

Transformation of the diameter change waveform into a pressure pulse is accomplished by using the equation given below.

$$EP(t) = P_{min} + [((E(t) - E_{min})(P_{max} - P_{min}))/(E_{max} - E_{min})] \qquad (A.3)$$

where EP(t) is the instantaneous pressure calculated from the UET data.